SCIENCE CHINA
Earth Sciences

•REVIEW•

July 2020 Vol.63 No.7: 899–918
https://doi.org/10.1007/s11430-019-9595-8

Metallogenesis and major challenges of porphyry copper systems above subduction zones

Huayong CHEN[*†] & Chao WU[†]

Key Laboratory of Mineralogy and Metallogeny, Guangzhou Institute of Geochemistry, Chinese Academy of Sciences, Guangzhou 510640, China

Received June 10, 2019; revised February 5, 2020; accepted February 24, 2020; published online April 3, 2020

Abstract Porphyry copper±molybdenum±gold deposits (PCDs) are the most representative magmatic-hydrothermal metallogenic system above subduction zones with important economic value. Previous studies revealed that large PCDs are generally formed from initial arc magmas (from subduction-induced partial melting of the mantle wedge), which eventually ascend to the shallow crust (3–5 km) for mineralization after a series of complex evolution processes. These processes include (1) the dehydration or partial melting of subducting slab, which induces partial melting of the metasomatized mantle wedge; (2) the ascent of mantle-derived magma to the bottom of the lower crust, which subsequently undergoes crustal processes such as assimilation plus fractional crystallization (AFC) or melting, assimilation, storage and homogenization (MASH); (3) the magma chamber formation at the bottom of the lower, middle and upper crust; (4) the final emplacement and volatilization of porphyry stocks; and (5) the accumulation of ore-forming fluids and metal precipitation. Despite the many decades of research, many issues involving the PCD metallogenic mechanism still remain to resolve, such as (1) the tectonic control on the geochemical characteristics of ore-forming magma; (2) the reason for the different lifespans of the long-term magmatic arc evolution and geologically "instantaneous" mineralization processes; (3) the source of ore-forming materials; (4) the relative contributions of metal pre-enrichment to mineralization by the magma source and by magmatic evolution; and (5) the decoupling behaviors of Cu and Au during the pre-enrichment. These issues point out the direction for future PCD metallogenic research, and the resolution to them will deepen our understanding of the metallogenesis at convergent plate boundaries.

Keywords Subduction zone, Porphyry Cu deposit, Metallogenesis

Citation: Chen H, Wu C. 2020. Metallogenesis and major challenges of porphyry copper systems above subduction zones. Science China Earth Sciences, 63: 899–918, https://doi.org/10.1007/s11430-019-9595-8

1. Introduction

Porphyry copper±molybdenum±gold deposits (PCDs) have critical economic value: For nearly a century, they have supplied nearly 3/4 of the world's copper, 1/2 of the molybdenum and 1/5 of the gold, as well as large amounts of silver, zinc, tin and tungsten (Sillitoe, 2010; Sun et al., 2015). The PCDs consists of porphyry copper-molybdenum and copper-gold deposits (Sillitoe, 1997; Hou et al., 2004; Hou and Yang, 2009; Sillitoe, 2010). PCDs are mostly spatially and genetically associated with shallow, intermediate to acid, porphyritic intrusions (Zhai et al., 2011). PCDs usually have large reserves, shallow burial depths and are easily mined, which make them the key deposit type in the industry. As many world-class copper deposits are PCD-type, the physicochemical mechanism and geodynamic background of PCD formation have long been a hotspot of ore deposit research.

At present, the PCD metallogenic mechanism covers the following key aspects: (1) The ore-forming magmas were sourced from the mantle wedge above the subducting oceanic crust, and then ascent to the bottom of the lower crust; (2)

* Corresponding author (email: huayongchen@gig.ac.cn)
† Contributed equally to this work

magma evolution from the bottom of lower crust to the magma chamber(s) in the middle and upper crust; (3) magmatic-hydrothermal processes of fluid phase differentiation caused by the intrusion emplacement in the upper crust; and (4) formation, migration and ore precipitation of the ore-forming fluids (Mungall, 2002; Richards, 2003; Candela and Piccoli, 2005; Sillitoe, 2010; Wilkinson, 2013; Blundy et al., 2015; Sun et al., 2015; Zhang and Audétat, 2017). Based on previous studies, we systematically summarized the PCD metallogenic mechanism from the deep magma sources to the shallow hydrothermal processes, clarified certain key unsolved issues and future research directions of the PCD formation, so as to further refine the PCD metallogenic model at convergent plate boundaries.

2. Overview of PCD ore formation above plate subduction zones

2.1 From subducting slab to partial melting of mantle wedge

Large PCDs worldwide are mainly distributed in subduction boundaries (e.g., island/continental arcs), and the ore-forming parental magmas are closely subduction-related, especially those formed by partial melting of subducting slab or mantle wedge triggered by slab dehydration (Mungall, 2002; Richards, 2003; Cooke et al., 2005; Sillitoe, 2010; Sun et al., 2011; Sillitoe, 2018; Figure 1). According to some conventional models of arc magma formation, subducting slabs dehydrate at around 100 km depth in subduction zones (i.e., blueschist- and eclogite-facies transition zone), during which the water-soluble large ion lithophile elements (LILE: e.g., Rb, K, Cs and Ba) are added to the asthenospheric mantle wedge, while the high field strength elements (HFSE, e.g., Nb, Ta and Ti) remain in the rutile phase of the subducting slab (Tatsumi et al., 1986; Davidson, 1996). In addition, many studies have found that arc magmas (especially PCD-related ones) may have also sourced from direct melting of the subducting slabs (including overlying sediments). This often occurs in hot and young (<25 Ma) slabs with high buoyancy, and are typically characterized by the formation of adakites, most of which have negative HFSE anomalies and high Sr/Y ratios (Defant and Drummond, 1990). It is noteworthy that the partial melting of young oceanic crust is not the only mechanism for the formation of adakites rocks, and numerous studies have shown that the PCD mineralization in the Central Andes were resulted from partial melting of the thickened lower crust (Kay and Mpodozis, 2001; Bissig et al., 2003; Kay et al., 2005; Sillitoe and Perelló, 2005). The dehydration/melting mechanism of the subducting slab could reflect the changing behavior of oceanic crust with depth. At shallow depth, dehydration of the subducting oceanic crust and sediments play a dominant role. As the depth increases, the oceanic crust undergoes eclogite-facies metamorphism and starts to melt (Wilkinson, 2013). The slab-derived fluids in the shallow part (<90 km) of the subduction system mainly enter the leading edge of the island arc. Only when the oceanic crust is dehydrated and melted at great depth in the subduction zone, can it contribute to the magmatic activity in the island arc (Marschall and Schumacher, 2012; Zheng et al., 2016). Dehydration and melting are not two completely separated mechanisms. It is found that a supercritical fluid transition state (>180 km) exists between the silicate melt (formed by slab melting) and the fluid (formed by slab dehydration), and bear the features of both end-members. This explains the coexisting silicate and gas inclusions in diamond and mantle xenoliths (Schiano and Clocchiatti, 1994; Kessel et al., 2005), as well as significant Nb/Ta fluctuations in some island arc basalts (Chen et al., 2018). The supercritical fluid may have extracted Cu and Au from the mantle wedge into the PCD-forming island arc magma (Mungall, 2002).

Dehydration of oceanic crust in the subduction zone is more common than slab melting (Pearce et al., 2005). The fluids derived from subducting slab (serpentine and brucite) dehydration entered the overlying asthenospheric mantle wedge (Grove et al., 2002; Hattori and Guillot, 2003), and the metasomatized mantle peridotite formed new hydrous minerals (e.g., amphibole and mica) that lowered the mantle solidus temperature and caused partial melting (Tatsumi et al., 1986). During the partial melting of the asthenospheric mantle rocks, if rutile is present in the melt residuals, "wet", HFSE-depleted and LILE-enriched high-Al basaltic melt (Al_2O_3>16 wt.%) would be generated. These geochemical features are likely inherited from the asthenosphere metasomatized by subducting fluids (Richards, 2003; Candela and Piccoli, 2005). In the subduction system, compositions of the slab-derived fluids vary with depths: It is considered that at several kilometer depths, elements such as Cl, S, and B in the seawater are temporarily incorporated into the serpentinite by intense metasomatism (Kerrick and Connolly, 2001; Pagé et al., 2018), and formed the fluid-rich oceanic crust dehydration reaction (Kent et al., 2002). However, as the depth increases, the salinity of the dehydrated fluid gradually decreases after reaching the peak. For example, the melt inclusion Cl/H_2O ratios of olivine from the Central American volcanic arc rise to a maximum and then decreases gradually from the volcanic front to the back-arc basin (Walker et al., 2003; Candela and Piccoli, 2005). Similar studies also found that the ratios of B/La, As/Ce, Pb/Ce and Sb/Ce decrease sharply from the volcanic front to the back-arc basin, suggesting that the lithophile elements (e.g., Pb, As, Sb and B) migrate by anionic complexes (HS^- and Cl^-) in the fluids. The key controlling factor for such spatial distribution of fluid-mobile elements is the progressive metamorphism in the subduction zone, which leads to the gradual

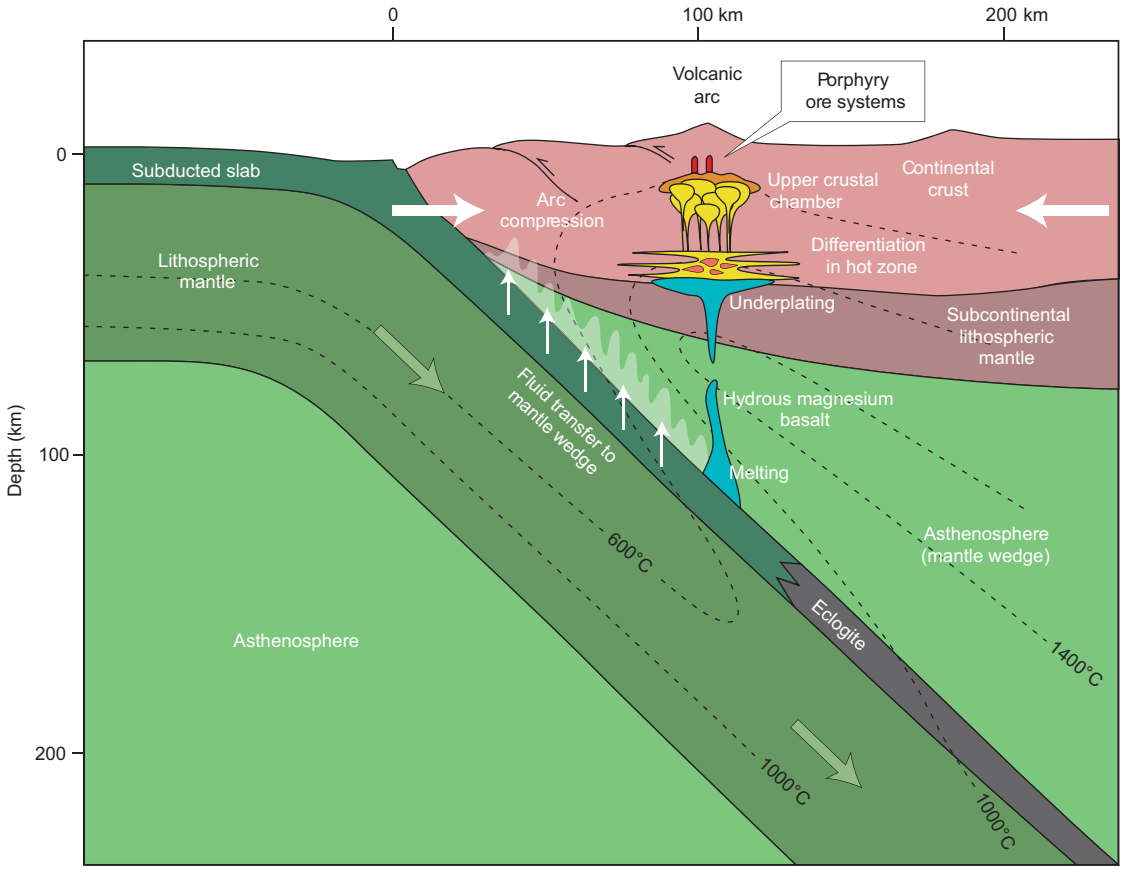

Figure 1 PCD metallogenic model above the subduction zone. Modified from Wilkinson (2013).

release of elements from the subducting slab (Leeman, 2001). Although simulation studies suggested that the addition of slab-derived fluids into the mantle is accompanied by sharp pH fluctuations, which increase the metal solubility and promote metal transport (Galvez et al., 2016), certain metal contents (e.g., Cu and Zn) and ratios (W/Th, Sn/Sm and Mo/Ce) of the volcanic arc show no systematic changes, indicating that these elements are not transported by the early slab-derived fluids (Noll et al., 1996). Both fluid- and melt-induced metasomatism can form hydrous minerals (e.g., phlogopite, amphibole) and other minerals (e.g., clinopyroxene and apatite) in the mantle wedge, yet the fluid-induced metasomatism introduces soluble LILEs (Wilkinson, 2013), while the melt-induced metasomatism introduces HFSEs (Bodinier et al., 2004). It is considered that the melt generated by slab partial melting removes Be and Th from the mantle, but introduces substantial Fe^{3+} and light rare earth elements (LREEs) into it (Kessel et al., 2005).

There are two views on the slab influence on oxygen fugacity (fO_2) of the mantle wedge: The first viewpoint suggests the slab-derived fluid or melt adds CO_2, H_2O, Fe^{3+} and other oxidized components to the mantle, thereby increasing the fO_2 of the metasomatized mantle (Mungall, 2002; Kelley and Cottrell, 2009). The partial melting products of the mantle wedge with high fO_2 are represented by "wet" high-Al basalts, whose sulfur exists mainly as sulfates. This enables the chalcophile elements (such as Cu and Au) to accumulate in the melt phase during the magma evolution (Richards, 2003). It takes 25% partial melting of the mantle to extract all the sulfide phases. However, if the mantle is hydrated and oxidized by slab-derived volatiles, all sulfides can be extracted by merely 6% of partial melting (Jugo, 2009). Moreover, the Fe^{3+} solubility in the melt is 400 times higher than that of the fluid, and therefore the melt can significantly increase the fO_2 (and thus sulfide solubility) of the mantle, which is conducive to PCD formation (Mungall, 2002). The second view proposes that the subduction does not make the sub-arc mantle more oxidized (Dauphas et al., 2009; Jenner et al., 2010). These studies found that Cu, a redox-sensitive element, has similar contents in the primary arc magma (50–90 parts per million, ppm) and mid-ocean ridge basalt (60–70 ppm), suggesting that their respective mantle source have similar fO_2 (ΔFMQ=0–1; Lee et al., 2012). High fO_2 of the arc magma may be achieved by magmatic evolution in the crust (e.g., MASH process; Lee et al., 2012).

The above processes can be summarized as follows (Zheng et al., 2015): (1) subduction: Oceanic crust and overlying sediments subduct into the asthenospheric mantle. (2) De-

hydration/melting: During the eclogite-phase metasomatism, the oceanic crust is heated by the overlying mantle wedge, which causes significant metamorphic dehydration or partial melting. The dehydration produces fluids that are rich in LILEs, LREEs and Pb, but poor in HFSEs and HREEs. If the subducted slab is partially melted at depth, the decomposition of rutile phase and the remaining of garnet phase would produce felsic melts enriched in LILEs and LREEs, undepleted (or even partially enriched) in HFSEs, but depleted in HREEs and Pb. (3) Reaction: In the oceanic subduction tunnel, the fluid or melt reacts with the overlying mantle peridotite and locally forms an enriched mantle source. (4) Storage: Partial melting may not occur just after the formation of metasomatized mantle, but probably after a period of several years to billions of years. (5) Heating: The mantle wedge is heated by mantle convection, which causes partial melting of the metasomatized mantle, and the melt further ascends and evolves to alkaline to calc-alkaline basaltic melts.

2.2 Mixing of mantle and crustal magma in the lower crust

The primary basaltic arc magmas generated by partial melting of the mantle ascend to the surface mainly in the form of tholeiitic volcanism in some immature and thin island arc environments. Otherwise, the magmas rise and underplate the bottom of the thickened lower crust, and drive a series of complex crust-mantle interactions (DePaolo, 1981; Hildreth and Moorbath, 1988), including partial melting, assimilation, storage, and homogenization (Figure 2). Partial melting of the lower crust is induced by the emplacement and crystallization of the mantle-derived magma in the hot zone. The mantle-derived magma likely assimilates the crustal melt and experiences storage and homogenization to form the low-density andesitic-dacitic, neutral/acidic melt (DePaolo, 1981; Hildreth and Moorbath, 1988; Schilling and Partzsch, 2001), whose composition would continue to evolve via crustal assimilation and fractional crystallization (AFC) when the melt further ascends (Hildreth and Moorbath, 1988). However, this does not change the major geochemical characteristics formed in the MASH zone, e.g., high Sr content, LREE/HREE ratio, HFSEs and enriched Sr-Nd isotopes (Hildreth and Moorbath, 1988).

The MASH zone in the lower crust is commonly featured by periodic injection of "wet" mantle-derived basalts during its evolution, so as to accumulate abundant volatiles and metals for the PCD formation (Wilkinson, 2013). The H_2O range of the primary arc magma (high-Al basalt) is 1.2–2.5 wt.% (Sobolev and Chaussidon, 1996), while in the amphibolite-stability field intermediate magmas are of high-water content and low temperature (Müntener et al., 2001). Obviously, the water content of the primary arc magma cannot stabilize the amphibolite phase and falls in the plagioclase-stability field (Figure 3), thereby forming the normal island arc magmas that have no adakitic features. However, when the water content in the arc magma reaches >10 wt.%, it shifts from the plagioclase-stability field to the amphibole-stability field, which inhibits plagioclase crystallization but promotes amphibole crystallization (Figure 3). Since the

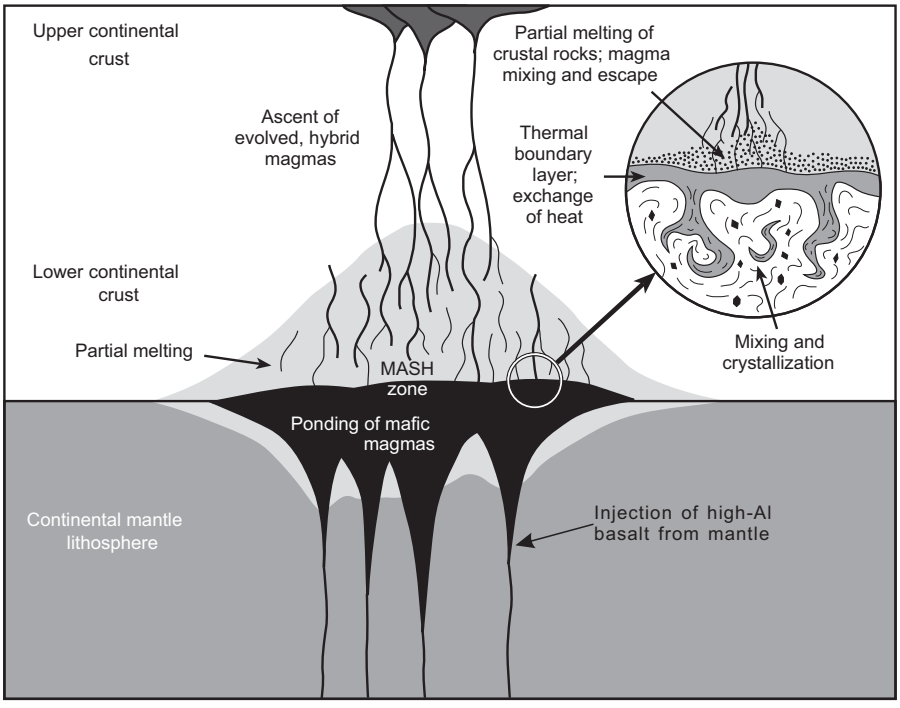

Figure 2 Schematic diagram of the MASH zone in the lower crust. After Richards (2003).

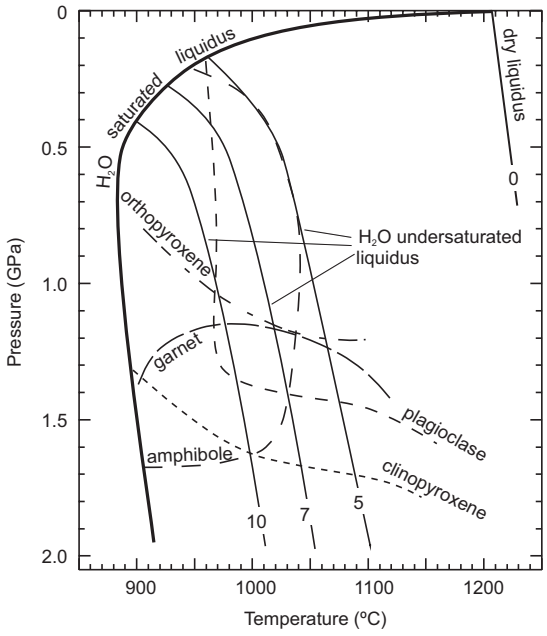

Figure 3 Pressure-temperature diagram, showing the liquidus for andesitic magma in the crust. The 5, 7 and 10 wt.% H_2O liquidus for plagioclase, amphibole, garnet, orthopyroxene, and clinopyroxene are marked with dashed lines. After Annen et al. (2005).

partitioning coefficient of La between amphibole and melt is lower than that of Yb, and that of Sr between plagioclase and melt is higher than that of Yb, adakitic or adakite-like magmas commonly have high Sr/Y, La/Yb, Sr (≥400 ppm), low Y (≤18 ppm) and Yb (≤1.9 ppm) contents (Kay, 1978; Defant and Drummond, 1990; Castillo et al., 1999).

The high water content of the melts in the MASH zone would also promote the crystallization of mafic minerals, such as olivine, pyroxene and spinel, and forms ultramafic cumulates at the bottom of the lower crust. This chemical discontinuity may form the Moho with discontinuous seismic velocity (Hildreth, 1981; Richards, 2003; Ducea et al., 2015). It is estimated that the middle and lower crust (with 50 wt.% amphibolite-facies rocks) act as a "sponge" that stores 20 wt.% H_2O in the arc magmas (Davidson et al., 2007). Studies show the occurrence of Fe-Ni-bearing sulfide melt or crystalline phase in the cumulates (Jagoutz et al., 2007; Hou et al., 2017). These sulfide droplets are captured due to their high density, and they usually have high Au, Cu and Au/Cu ratio, and are thus considered as the precursor of Au-rich PCDs in the mature arcs (Davidson et al., 2007), as well as PCDs related to post-subduction alkaline magmatism (Richards, 2009; Hou et al., 2017).

2.3 Magma migration in the crust, and the formation and evolution of magma chamber in the upper crust

Parental magma for PCDs formed in the MASH zone would ascend to the magma chamber at the bottom of the upper crust and then further evolves (Petford et al., 2000; Richards, 2003; Seedorff et al., 2005). It is generally considered that magmas rise slowly via diapir or magmatic erosion in the middle and lower crust. After crossing the brittle-ductile transition in the middle crust, the magmas may have intruded as dikes along preexisting faults and channels in the brittle wallrocks (Petford et al., 1993; Weinberg and Podladchikov, 1994; Petford et al., 2000; Richards, 2003; Seedorff et al., 2005). Some studies suggested that large faults (which extend to the lower crust) are important channels for the magma ascend (Glazner, 1991), which is conducive to the dike emplacement. Geophysical surveys revealed magma channel stockwork in the Andean continental arc, suggesting that the "wet", low-viscosity andesitic-dacitic magma generated in the MASH zone tends to emplace as dikes along the vertical normal faults formed by subduction and strike-slip shearing (Glazner, 1991; Schilling and Partzsch, 2001).

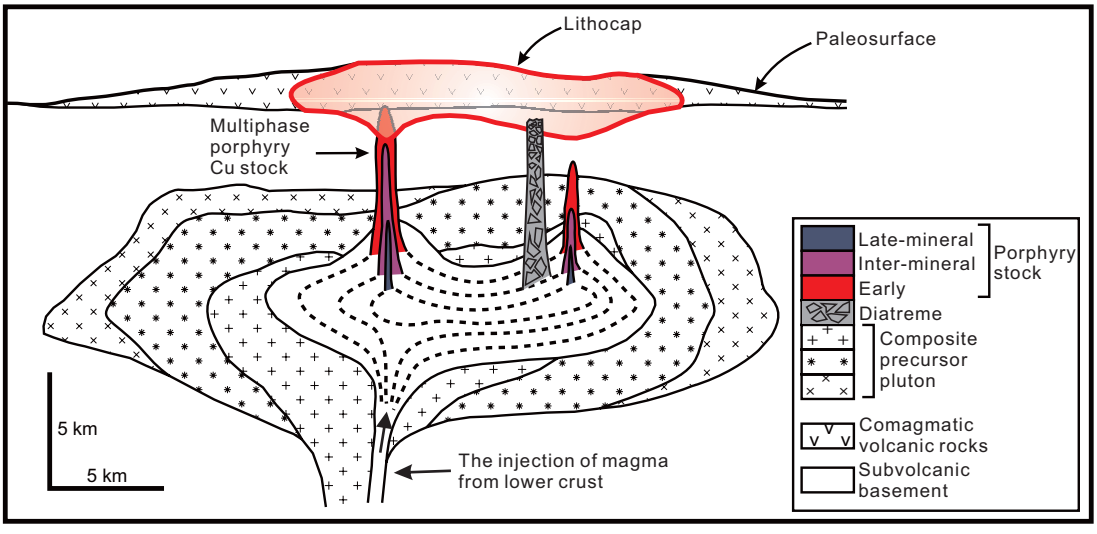

Figure 4 Schematic diagram showing the evolution of magma chamber in the upper crust. Modified from Sillitoe (2010).

Generally, the compressive tectonic background would lead to crustal thickening, which is conducive to the MASH process in the lower crust, but this excessively compressive stress would shut down the channel and stop magma ascent in the middle and upper crust (Richards, 2003). Meanwhile, the extensional tectonics (e.g., normal faulting) would facilitate the mafic magma to erupt directly onto the ground surface, which is unfavorable to mineralization (Luhr, 1997). Therefore, abrupt stress relaxation above subduction zones after long compression, or compression to extension transition, may be most favorable to generate the PCD-forming magmas (Richards, 2003).

The parental intermediate-felsic magma does not rise directly to the surface, but reaches the neutral buoyancy in the upper crust and experiences fractional crystallization, magma replenishment, and fluid exsolution in the magma chamber(s), whose volume would determine the tonnage of PCDs (Richards, 2003; Candela and Piccoli, 2005; Sillitoe, 2010), e.g., geophysical surveys revealed a magma chamber of nearly 2000 km^3 at 5–15 km deep below the Bingham deposit (Steinberger et al., 2013). The magma chamber in the upper crust is likely an open system (Figure 4): Magma can be supplied from the bottom and intruded as apophysis, stock and dike, or erupted as volcanic rocks (Candela and Piccoli, 2005). Intrusive magmatic activity depends on the physical properties of the magma chamber(s), such as the replenishment rate, the upper crustal strain rate, and the magma density and viscosity (Petford et al., 2000). At present, it is generally believed that when the new magma pulses intrude into the magma chamber from the bottom, the decompression and the consequent fluid exsolution leads to the formation of melt with abundant bubbles, which then rises to the magma chamber roof due to its lower density. On the roof, the volatilized bubbles are released from the melt due to the pressure drop, and the denser melt is subsequently pushed aside and then downward by the rising magma below, and eventually consolidate to form the batholith (Shinohara et al., 1995; Lowenstern, 2001; Candela and Piccoli, 2005).

Such convection in the magma chamber continuously carries ore-forming materials to the magma chamber roof, and the extensive volatilization is critical for the enrichment of ore-forming materials in the magma (Shinohara et al., 1995; Candela and Piccoli, 2005). Such extensive degassing commonly occurs when magma is injected into the magma chamber from the bottom, where the volatiles comprise initially CO_2 and SO_2 but becomes gradually H_2O-dominated during their ascent (Lowenstern, 2001). Therefore, the Au, Cu and other ore-forming elements in the melt tend to combine with S to form and migrate as complexes (Pokrovski et al., 2008). When these volatiles are introduced into the shallow level by faults in the magma chamber roof, the ore-forming elements may be pre-enriched in the wallrocks before the PCD formation, and may form mesothermal or epithermal Au deposits (Chiaradia et al., 2012). The volatiles may also mix with the groundwater to form acidic alteration closely spatially-related to porphyry and epithermal mineralization (Wilkinson, 2013). Besides, sulfide saturation in the magma chamber has also important effects on PCD mineralization: Saturation of magmatic sulfide under low temperature would generate sulfide crystals, but would form immiscible sulfide melt phase under high temperatures (Wilkinson, 2013), both of which would concentrate more Fe and Au than Cu, Pb, Zn and Ag (Peach et al., 1990).

The mechanism of sulfide saturation remains unclear, including the questions on the magnetite crystallization and the assimilation of reduced crustal materials, which may lower the magma fO_2 and cause sulfide precipitation (Ishihara and Matsuhisa, 1999; Jenner et al., 2010; Smith et al., 2012; Sun et al., 2015), as well as the influence of magma mixing (Keith et al., 1997; Halter et al., 2005; Wilkinson, 2013; Large et al., 2018). The lifespan of a magma chamber varies from 100000 years to 5 million years (Petford et al., 2000; Schoene et al., 2012), during which batch injections of mafic magma may occur (Glazner et al., 2004). Such episodic magma injections may not only induce porphyry emplacement and/or volcanic eruptions (Sparks and Marshall, 1986), but also lead to sulfur oversaturation in the andesitic magma produced by mixing of basaltic and dacitic magmas in the chamber (O'Neill and Mavrogenes, 2002; Halter et al., 2005), thus forming independent sulfide phases. It is noteworthy that in addition to direct mixing, mafic magma may also add volatiles into the magma chamber(s) to transform the textures of early-formed minerals in the chamber (Figure 5; Blundy et al., 2015). The Alumbrera Au-rich PCD (Argentina), for example, contains zircons with dark bands (CL image), which indicates disequilibrium crystallization triggered by volatile release from the replenished mafic magma (Buret et al., 2016). Volatiles from mafic magmas are characterized by having high temperature, high CO_2 and low H_2O contents, which may corrode the quartz crystallized from the

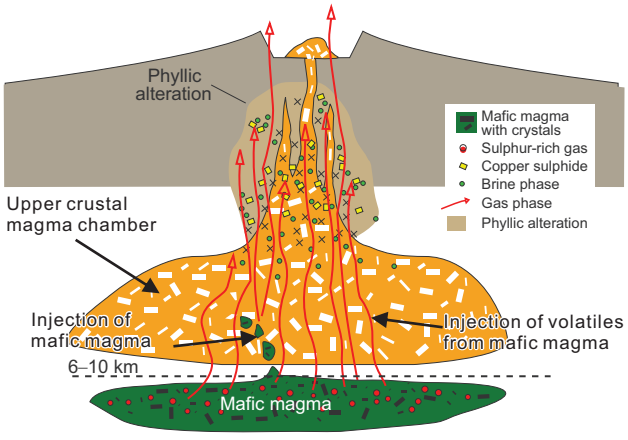

Figure 5 Schematic diagram illustrating mafic components recharging in the upper crustal magma chamber(s). Blundy et al. (2015).

lower-temperature felsic magmas (Wark et al., 2007).

2.4 Emplacement of ore-forming porphyries and volatile exsolution

Magma originated from the chamber at the bottom of the upper crust is emplaced in the upper crust as stock or apophysis, forming various mineralized porphyries. During the rapid ascend of mineralized intrusion from the magma chamber roof (ca. 5–15 km deep) to its final emplacement depth (ca. 3–5 km), the rapid decompression may have formed the cryptocrystalline groundmass, which (with the phenocrysts crystallized at depth) form the typical porphyritic texture (Candela and Piccoli, 2005; Sillitoe, 2010). It is noteworthy that the scale of the PCD mineralization is not necessarily related to the size of the ore-forming porphyry or the duration of magmatism (Sillitoe, 2010). When the pressure in the stock or underlying magma chamber is greater than the total lithostatic pressure, volatile exsolution (also known as "first boiling") occurs (Robb, 2009). The causes of unbalance between internal and external pressure may lead to the collapse of the upper volcanic edifice (Sillitoe, 1994), large earthquakes (Davis et al., 2007), rapid uplift and wallrock erosion (Sillitoe, 1994), brittle-ductile transition (Fournier, 1999; Ingebritsen, 2012; Weis et al., 2012) and mafic magma recharge (Caricchi et al., 2014). The rapid pressure release in the early-stage porphyry emplacement can also form breccia pipes, which can be mineralized, especially when the metals are not dispersed by eruption. For example, El Teniente (the world's largest PCD) is mineralized in magmatic-hydrothermal breccias, which contain biotite, anhydrite and tourmaline (Candela and Piccoli, 2005).

"First boiling" is vital for hydrothermal mineralization. The initial fluid is single-phase, low-salinity (H_2O-rich), which fractionates into a major low-density gas phase and a minor brine phase during ascending (Rusk et al., 2004; Sillitoe, 2010). The early single-phase volatiles are supercritical (Candela and Piccoli, 2005) and rich in ore-forming elements. Subsequently, the brine phase (salinity up to 35–70 wt.%) formed by phase separation of supercritical fluid (or direct exsolution from the magma) tends to be rich in Fe, Zn, Pb, Mn, and Mo, while the low-density gas-phase tends to be rich in Cu, Au, Ag and S (Heinrich et al., 1999; Pokrovski et al., 2008). Some authors argued that metals such as Cu may diffuse into the vapor-rich inclusion along the c-axis of quartz crystals, resulting in high vapor phase content (Li et al., 2009; Zajacz et al., 2009; Seo and Heinrich, 2013). Meanwhile, experimental studies of synthetic inclusions show that the Cu-Au contents are higher in the brine inclusions than vapor ones (Simon et al., 2005; Lerchbaumer and Audétat, 2012). Although the ore-forming element contents in the brine phase are high, the overall mass of the liquid phase is lower than that of the gas phase, hence the relative mass of the ore-forming substances in the two phases is difficult to be determined. It is generally believed that Mo is mainly transported in the brine phase, whilst Au (and half of the Cu) is mainly transported in the gas phase (Zajacz et al., 2017). This indicates that Au tends to form epithermal mineralization with gas-phase migration (Heinrich et al., 2004).

Studies on the elemental migration behavior in hydrothermal fluids found that Cu and Au are usually transported in chlorite complexes (Holland, 1972; Candela and Holland, 1986), while Mo is usually transported in H_2MoO_4 (under low salinity) or MoO_2Cl^+ (under high salinity) complexes (Yokoi et al., 1993; Ulrich and Mavrogenes, 2008). Other studies revealed that Cu and Au may also be transported as bisulfide complexes (Nagaseki and Hayashi, 2008; Pokrovski et al., 2008). Further simulations show that Cu tends to migrate in Cl^- complexes under low temperatures, but in HS^- complexes under high temperature (>300°C), which is resulted from the gradual sulfur content rise via the dissolution of pyrite and pyrrhotite (Zhong et al., 2015). In addition to temperature, salinity (Cl/H_2O) may be another influence factor on the metal migration behaviors: Under high Cl/H_2O, $D^{Au}_{fluid/melt}$ is positively correlated with Cl/H_2O value, indicating that Au forms complexes with Cl^-. Under low Cl/H_2O, $D^{Au}_{fluid/melt}$ is stable (close to 40), suggesting that Au may migrate in OH^- complexes (Frank et al., 2002; Simon et al., 2005).

2.5 Hydrothermal alteration and mineralizing processes

Although porphyry bodies are generally small, PCDs usually develop hydrothermal alteration zones that extend for several kilometers around the mineralization center (Figure 6a). Therefore, accurate delineation of alteration zones can greatly improve PCD exploration (Sillitoe, 1997, 2010). Lowell and Guilbert (1970) first proposed a bell-shaped alteration zone from the mineralization center: Potassic zone in the core, phyllic zone in the middle, propylitic zone in the periphery and argillic zone on the top. As the main mineralization zone, the potassic zone is one of the earliest in PCD formation and generally occurs at the top of the intrusion. The potassic zone comprises the mineral assemblage of K-feldspar, quartz, biotite, and magnetite. Propylitic alteration coeval with potassic alteration can extend for several kilometers away from the mineralization center, with mineral assemblage of chlorite, epidote, calcite, sodic feldspar, actinolite and pyrite, and consists of the actinolite-, epidote- and chlorite-bearing subzones (Cooke et al., 2014). Sericite alteration has the mineral assemblage of sericite, quartz, chlorite, and pyrite. It is important to note that, unlike the early alteration zoning model (which has phyllic alteration

distributed as annulus separating the potassic and propylitic zones; Lowell and Guilbert, 1970), phyllic alteration is commonly structurally-controlled and overprint the early potassic and propylitic zones (Sillitoe, 2010). The argillic zone, generally distributed above the other alteration zones, has the mineral assemblage of quartz, kaolinite, illite, pyrophyllite and alunite. Argillic alteration often superimposes on the early alteration zones, and gradate from a shallow quartz-pyrophyllite subzone to a deep sericite zone (Sillitoe, 2010).

Physicochemical characteristics of the hydrothermal fluids in the different alteration zones also vary: The potassic alteration fluids are initially of high-temperature and single-phase, and segregates into the high-density brine phase and low-density gas phase during ascending (Rusk et al., 2004). Volatiles for the phyllic stage are low-temperature liquid phase directly differentiated from the magmas (Sillitoe, 2010). The propylitic alteration fluid is formed by mixing the magmatic-sourced brine with the circulating groundwater heated by the intrusions (Cooke et al., 2014). It is noteworthy that there are two argillic alteration stages: The early stage coincides with the potassic stage, and is produced by the low-density vapor phase that rises and injects into the top of the alteration zone; The late-stage originates from the low-temperature fluid of the phyllic alteration (Sillitoe, 2010). In summary, the potassic and the coincident argillic alteration are produced by magmatic-hydrothermal fluids, and the propylitic alteration is derived from mixing different proportions of the magmatic and meteoric fluids. Therefore, although coincident with the potassic alteration, the propylitic alteration may still overprint the latter when the hydrothermal system gradually waned and invaded by the meteoric water (Sheppard, 1977; Richards, 2018). The phyllic and the corresponding argillic alteration are still dominated by the low-temperature hydrothermal fluids (Hedenquist et al., 1998), with more meteoric addition toward the peripheral zone (Fekete et al., 2016). However, some studies argued that meteoric water is not a prerequisite for the phyllic alteration (Harris and Golding, 2002).

Hydrothermal veins, which have consistent symbiosis and crosscutting relations in different PCDs, are good record of PCD-type hydrothermal activities (Figure 6b; Gustafson and Hunt, 1975; Sillitoe, 2010; Richards, 2018). The earliest veins include EDM veins, with the mineral assemblage of quartz+sericite+K-feldspar+biotite+chalcopyrite±bornite with clear alteration halo. Sinuous A veins have the mineral assemblage of quartz+K-feldspar+anhydrite+sulfide with no alteration halo, while the actinolite-, magnetite- (M veins), biotite- (EB veins) or K-feldspar-dominated veins all lack quartz or sulfides. These early veins are formed by the high-temperature potassic alteration fluids, and are usually weakly mineralized. The EDM veins may represent the earliest single-phase volatiles, while the A veins represent the vapor and liquid phases of volatiles (Rusk et al., 2008). The straight B veins (which cut the early veins) have the mineral assemblage of quartz+anhydrate+chalcopyrite+molybdenite with narrow or fuzzy alteration halo, and are formed by the relatively low temperature (450–350°C) vapor and liquid phases in the potassic alteration (Roedder, 1984). These veins contain disseminated sulfides that contribute to the main ore resource in most deposits (Sillitoe, 2010). Late D veins (which cut A and B veins) comprise mainly pyrite and chalcopyrite and minor quartz and anhydrite, and develop sericite halos via the alteration of feldspar (Pollard and Taylor, 2002). The D veins are formed in the phyllic alteration under low temperature (350–250°C), and can alter Cu sulfides and molybdenite precipitated in the potassic stage (Landtwing et al., 2005; Sillitoe, 2010; Richards, 2018).

Ore mineral precipitation can be triggered by many mechanisms, including temperature and/or pressure drop, and fluid-wallrock reactions, and other processes that can reduce the metal solubility (Ulrich and Heinrich, 2002; Landtwing et al., 2005; Williams-Jones and Heinrich, 2005; Rusk et al., 2008; Sillitoe, 2010). Although the solubility of ore-forming elements generally drops with decreasing temperature (e.g., chalcopyrite solubility drops sharply at 400–250°C; Crerar and Barnes, 1976), temperature drop alone is unlikely sufficient to generate a large PCD, given that the lifespan of upper crustal magma chambers in the upper crust can last for 100000 years, the mineralization is completed in a very short time period (high-flux sulfur in volcanic eruptions is enough to supply the huge amount of sulfur needed for PCDs in several decades). This suggests that efficient metal and sulfur precipitation cannot be satisfied only by the spontaneous cooling of a single magmatic fluid (Fournier, 1999). Therefore, the mixing of high-temperature magmatic-derived brine with circulating meteoric water (Henley and McNabb, 1978; Dilles, 1987) or magmatic volatiles has been proposed as an ore precipitation mechanism (Blundy et al., 2015). The mixing can reduce both temperature and salinity, thus decreasing the solubility of ore-forming materials (Henley and McNabb, 1978; Hedenquist and Lowenstern, 1994; Fekete et al., 2016). According to the mixing model with magmatic volatiles, the migration and precipitation of the ore-forming materials are not resulted from the continuous evolution of a single magma system. Instead, the S-poor and Cl-rich brine exsolved from intermediate-felsic magmas may have transported the ore-forming elements, and the sulfide precipitation is triggered by the interactions between the metal-bearing fluids and the H_2S-rich volatiles from the mafic magma injecting into the chamber(s) (Blundy et al., 2015).

Sulfides accumulate huge amounts of metals (Fe, Cu, Mo, and Au) and sulfur, e.g., El Teniente contains up to 1 Gt S, 200 Mt Cu, 2.5 Mt Mo and 2600 t Au (Wilkinson, 2013; Blundy et al., 2015; Zhang and Audétat, 2017). When the

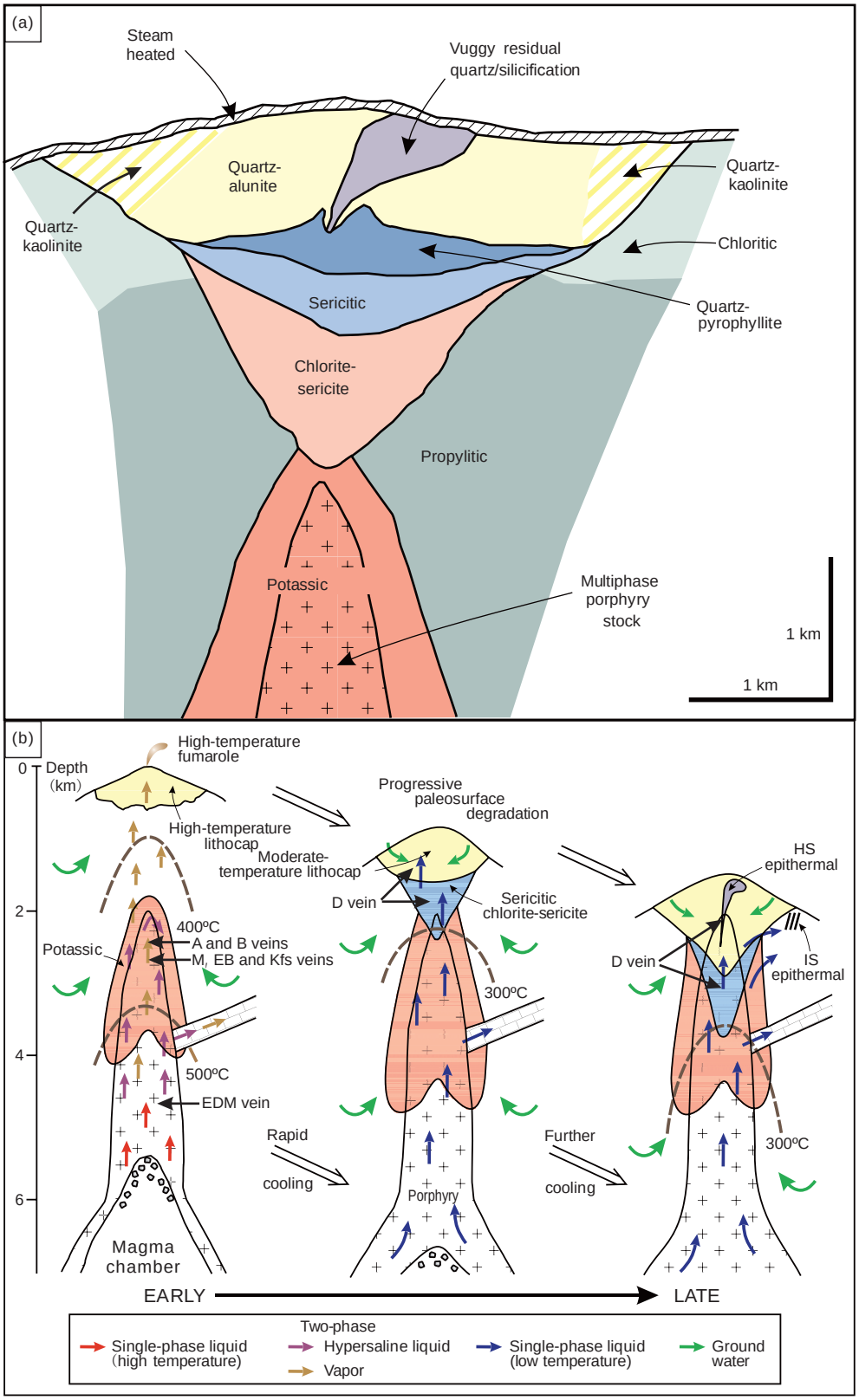

Figure 6 Schematic diagram of alteration zoning of typical PCDs (a) and its magmatic-hydrothermal evolution (b). Modified from Sillitoe (2010).

ore-forming elements migrate in the form of Cl^- complexes, large amounts of reductant are needed to precipitate the sulfides, via reduction of homologous oxidized S (SO_2 or SO_4^{2-}) or addition of external reduced S (Zhong et al., 2015).

Possible reduction mechanisms include magnetite crystallization and/or reaction with reductants in the wallrocks. The former is supported by the extensive magnetite occurrence in PCDs (Sun et al., 2015), while the latter is interpreted to account for the formation of large porphyry Cu-Au deposits such as Bingham and Grasberg (Wilkinson, 2013). When the metals migrate as HS-complexes in the fluids, the metal and S may have adequately supplied in the same magmatic-hydrothermal system (i.e., no extra S source needed), and the metal precipitation can be achieved through decomposition of HS-complexes triggered by H_2S degassing and/or reaction with the wallrocks (Qian et al., 2010; Zhong et al., 2015).

2.6 Comparison of tectono-magmatic and mineralization processes of PCDs in island and continental arcs

There are two major tectonic settings for PCD formation, i.e., island arc and continental arc (Sillitoe, 2018). PCDs formed in island arc setting, e.g., those in the Southwest Pacific (Uyeda and Kanamori, 1979; Harrison et al., 2018; Maryono et al., 2018), include the Far South East and Atlas (Philippines), the Batu Hijau and Tumpanpitu (Indonesia), and the Lihir porphyry and epithermal Au deposits (Papua New Guinea). PCDs formed in continental arc setting are best represented by those in the Central Andes, notably the Bajo de la Alumbera (Argentina) and El Teniente (Chile) (Uyeda and Kanamori, 1979).

Oceanic subduction tends to produce extensional arcs due to its commonly steep subduction angle, and is accompanied by the extensive development of back-arc basins. Many island arcs have thick accumulations of basaltic volcanic rocks on an oceanic crustal basement. Continental arcs are characterized by coastal mountain ranges and andesite layers, as well as accretionary wedges in their forearc (Uyeda and Kanamori, 1979). In general, the oceanic and continental lithosphere is 80–120 km and >100 km thick, respectively, thus the downgoing oceanic slab would encounter the asthenospheric mantle at >100 km deep beneath the arc (Zheng et al., 2016). The fluid or melt produced by the subducting plate ascends through the asthenospheric and lithospheric mantle, and finally enters the crust of the overlying oceanic island arc or continental arc. The mineralized porphyries in oceanic island arcs are mainly calc-alkaline dioritic, whereas those in the continental arcs are mainly high-K calc-alkaline (or shoshonitic) granitic, which reflects higher degree of fractionation when the magmas pass through the thicker continental crust in the latter (Hou, 2004).

Formed in a typical island arc setting, the Baguio porphyry Cu-Au district (Luzon, Philippines) is a key Cu-Au province in the world, the young (ca. 3.5 Ma) mafic and felsic magmatism is closely mineralization-related (Hollings et al., 2011). The felsic magmatism is low- to medium-K, adakitic and contaminated by young arc crustal materials, and underwent further fractionation in the shallow crustal magma chamber(s). Geochemical and isotopic characteristics of the mafic dikes are similar to those of the primary mantle-generated magmas, indicating that the mafic magmas experienced little crustal contamination through the crust of the arc (Figure 7). Formation of these mafic dikes was coeval with the subduction flattening, caused by the subduction of the Scarborough ridge. Moreover, considering that the Scarborough ridge is younger than the subducting slab, and therefore easier to melt, the melt generated by the former may have formed adakitic rocks in the Baguio area, and induced the mantle wedge to melt to form the primary mafic magma. Further petrological studies revealed the extensive magma mixing between the original mafic melt and felsic melt in the crust of the overlying island arc (Cao et al., 2018b): The original mafic magma contains high Cu contents (~600 ppm), and felsic magma (~300 ppm Cu), and provides

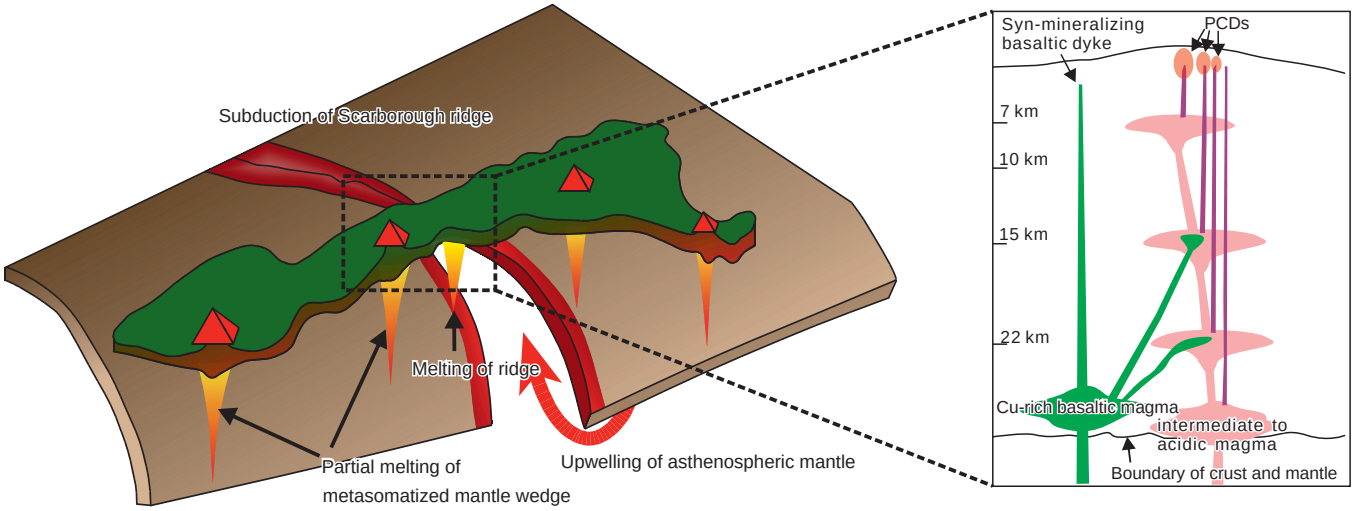

Figure 7 Tectonic-magmatic model of PCD formation in the Baguio area, Luzon (Philippines). Modified from Hollings et al. (2011) and Cao et al. (2018a).

abundant metallogenic materials for the PCD formation (Cao et al., 2018a; Figure 7).

A series of world-class PCDs are developed in the Central Andes bordering Chile and Argentina, e.g., Los Pelambres, Rio Blanco-Los Bronces and El Teniente (Cooke et al., 2005). During the early Oligocene to early Miocene, the Abanico basin was developed between the Coastal Range and Cordillera block, during which extensive volcanic rocks were deposited. In the middle-late Miocene, due to the subduction of Juan Fernandez ridge and/or the arc lithospheric migration to the accretionary wedge, flat-slab subduction occurred and the continental arc underwent intense compression, which halted the volcanism and closed the Abanico arc basin. During this period, minor magmatism was formed by partial melting of the lower crust. In the late Miocene to Pliocene, the continuous and extensive compression gradually thickened the arc crust, and the mantle magma rose into the MASH zone of the lower crust to form the ore-forming magma, and the final mineralization may have occurred along the thrust faults in the Abanico basin (Mpodozis and Cornejo, 2012; Figure 8).

Porphyry-type mineralization in this region is closely related to multistage amphibole-bearing intermediate intrusions from long-living magmatic system (>10 Ma; Perelló et al., 2012). The hydrous, oxidized and adakitic magma in this region was formed via (1) the fractional crystallization of amphibole in the MASH zone when the magma evolved to high water content (Davidson et al., 2007); (2) the lower crust is thickened to the critical value (45 km) and eclogite-phase metamorphism occurred under high pressure, i.e., the unstable hornblende phase is transformed into garnet, releasing water and other volatiles (Kay and Mpodozis, 2001).

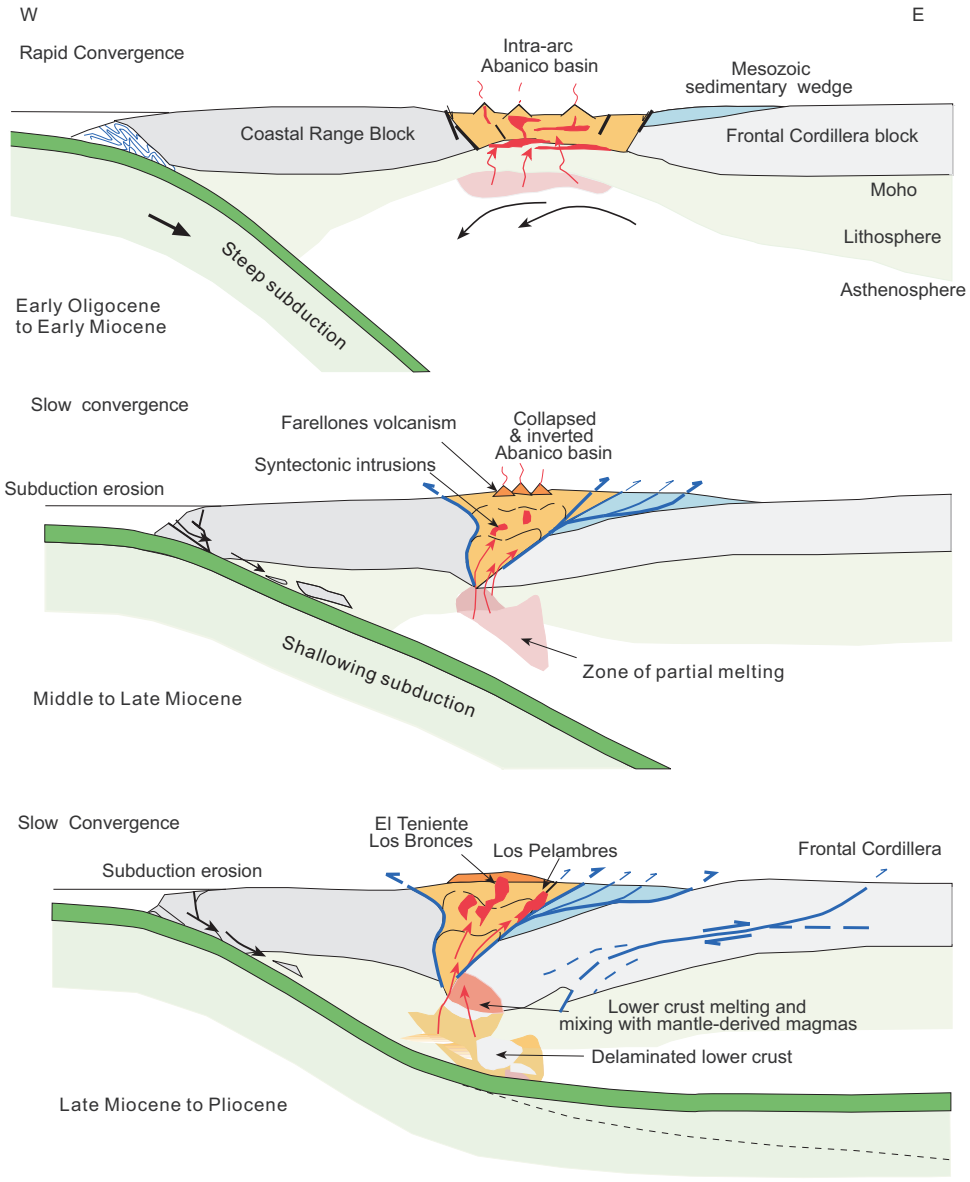

Figure 8 Schematic tectono-magmatic model for the PCD formation in the Central Andes. After Mpodozis and Cornejo (2012).

It is noteworthy that the flat-slab subduction also leads to intensive forearc erosion, which may also introduce water into the magmas (Stern et al., 2010). These mechanisms enrich the magmas with water, which is conducive to mineralization.

Comparing the PCD genetic models in typical island arc and continental arc settings, earlier studies considered that the adakites in the two settings have different magma sources (Zhang et al., 2001; Liu et al., 2004): Adakitic rocks in island arcs are originated from partial melting of the young and hot subducting slab. The partial melting is triggered by the asthenospheric upwelling induced by the break-off of subducting ridge, different from the adakites formed by partial melting of the thickened lower crust in continental arcs. In the Sr/Y vs. $(La/Yb)_N$ diagram, the adakites from the Pacific Rim mainly fall in the oceanic crust melting field, which is markedly different from the adakites of the thickened lower crust melting origin (Ling et al., 2011). This suggests joint contributions of the subducting oceanic crust (especially oceanic ridge) to the adakite formation in both island arc and continental arc settings. Although the island arc crust is generally thinner than the continental arc crust, mature island arcs still undergo evolution in the MASH zones, similar to continental arcs. For example, some studies suggested that forearc adakites in the Philippines may have originated from the MASH process at the bottom of the oceanic island arc crust (ca. 30 km deep; Ribeiro et al., 2016).

3. Major scientific issues and future research directions for PCD metallogenesis

Integrating the above analysis on the metallogenic regularities of major PCDs worldwide, existing PCD metallogenic questions can be summarized as the following three aspects: (1) Tectono-dynamic background and evolution of PCDs; (2) ore-forming material (e.g., Cu, Au, Mo) source; (3) efficient pre-enrichment mechanism of ore-forming materials in the crustal magma source.

3.1 Mineralization implications from tectono-magmatic background

Statistics show that a large number of ore-forming porphyries have adakitic characteristics (Oyarzun et al., 2001; Reich et al., 2003; Richards, 2003; Cooke et al., 2005; Chiaradia et al., 2012; Sun et al., 2015). The origin of adakites by partial melting of oceanic crust challenges the traditional understanding that the magma produced by partial melting of subduction plates cannot directly reach the surface due to the barrier of mantle wedge and crust, but suggests the existence of deep faults as the channels linking the lithosphere and the asthenosphere (Defant and Drummond, 1990; Reich et al., 2003). However, some studies put forward that geological processes such as partial melting of the lower crust (Wang et al., 2004) and the juvenile lithosphere (Hou et al., 2009; Sun et al., 2018), or fractionation of the normal arc magma (Castillo, 2006) may form the adakite-like geochemical characteristics. Experimental petrological studies also revealed that the partial melting of eclogite-facies metamorphosed subducting slab (with garnet residual) (Defant and Drummond, 1990) is not the only way to produce adakite-like geochemical features. The "wet" magma in the lower crustal MASH zone can directly enter the amphibole-stability field and plagioclase-decomposition zone to produce adakites (Richards et al., 2012). Previous studies have compared the adakites in the Middle and Lower Yangtze River Belt (MLYRB) and in the Dabie Orogen, which were formed by partial melting of oceanic crust in eastern China and the continental lower crust, respectively (Liu et al., 2010; Ling et al., 2011). These studies found that the MLYRB adakites have lower La/Yb (14–49 vs. 21–402), Th/U (0.3–8 vs. 2.3–51) and Nb/Ta ratios (7.5–23 vs. 5–65) than those in the Dabie Orogen.

The diversification of geological origin of adakite inevitably complicates the understanding of the tectono-metallogenic background. The PCDs are not only distributed in the island arcs, such as the Atlas, Grasberg and Batu Hijau Cu-Au deposits in the western Pacific (Cooke et al., 2005), but also in the continental marginal arcs, such as the El Teniente Cu-Mo and Alumbrera Cu-Au deposits in the Andes (Cannell et al., 2005), and collisional orogenic belts, such as the Qulong Cu-Mo deposit in Tibet (Hou and Yang, 2009). With the adakitic source shifting from the oceanic crust to the lower crust or Subcontinental Lithospheric Mantle (SCLM) (Richards et al., 2012; Griffin et al., 2013), the water-rich nature of the magma source in the lower crustal MASH zone would play a more prominent role in controlling PCD mineralization. The MASH model was first proposed to explain the formation of normal arc magma (Hildreth and Moorbath, 1988), and magmas in the MASH zone evolve gradually to become more water-rich, which is difficult to explain the sporadic and scarce PCD distributions in the arc magma, or the coexistence of ore-forming and ore-barren porphyries in the same tectonic setting. In addition, the MASH process is based on studies on the Andean arc with significant crustal thickening. It is worth considering that (1) whether there is any difference in the MASH process between the thicker continental arc crust and the thinner oceanic island arc crust; (2) would subduction directly supply magmas that are rich in ore-forming materials, or are the magma fertilized by magmatic evolution in the crust; (3) whether there are any geochemical indices that can determine the MASH processes, including the initiation of the island arc crustal thickening, progressive metal concentration and eventual mineralization.

The long-term evolution of the magmatic arc and in-

stantaneous mineralization are other key issues in the study of PCD tectono-dynamic setting. Arc magmatism has commonly a long lifespan. For example, the coastal batholiths in NW America were formed over a period of 160 Myr (from 210 to 50 Ma; Ducea et al., 2015). It may take tens of thousands of years to establish an effective magma pumping system that connects the lower and upper arc crust (Whattam and Stern, 2016), and it may take 10000 years to 1 Myr to form a batholith-scale magma chamber in the middle and upper crust (Ardill et al., 2018). High-precision geochronological studies revealed that the Haquira East PCD (Peru) was formed within 35000 years (Cernuschi et al., 2018), indicating that the mineralization lifespan was mostly shorter than 100 kyr. In terms of the lifespan of a single hydrothermal alteration stage, the phyllic alteration veins of the Butte PCD (United States) were formed within 100 years, whilst the potassic alteration occurred within 900 years (Geiger et al., 2002). Simulation reveals that the alteration halo of potassic veins in the Alumbrera PCD (Argentina) were formed in 20 years (Cathles and Shannon, 2007), which suggests that a single alteration stage can occur within hundreds of years.

Compared to the formation of magma chambers and island arcs that lasted for over millions of years, both the century-scale single-stage veining and the thousand-year-scale hydrothermal mineralization event are geologically instantaneous. Therefore, mineralization is unlikely to be continuous with slow exsolution of magmatic volatiles in a passive state, because such slow degassing of hydrothermal volatiles accompanied by the gradual cooling and magma crystallization is a continuous, million-year-scale process in the magma chambers (Sparks and Cashman, 2017). Moreover, this passive degassing of magmatic-hydrothermal fluid may be accompanied by cooling via mixing with groundwater, which forms weak propylitic alteration with rare mineralization (Richards, 2018). Meanwhile, massive volcanic eruptions in the magmatic arcs may have triggered the formation of large PCDs. For example, the metal contents in the volcanic gas from the Merapi volcano (Indonesia) during eruptions are several orders of magnitude above those in the intermittent volcanic gas (Nadeau et al., 2010). The metal ratio of the volcanic gas is close to that in the sulfide of the erupted lavas, suggesting that the volcanic eruption promoted sulfide decomposition by volcanic gas and the extraction of ore-forming materials, which is conducive to rapid PCD formation. Some studies suggested that earthquakes over magnitude 9 and the possible subsequent volcanic edifice collapse may trigger such "instantaneous" porphyry mineralization (Nadeau et al., 2010; Richards, 2018). If accidental events are prerequisite to mineralization, it would undoubtedly greatly change our understanding of magmatic-hydrothermal process of PCD formation. However, the high metal contents in the Merapi volcanic gas only occurred in the eruption year (Nadeau et al., 2010), and the duration was far shorter than the centennial lifespan of a single alteration stage, let alone the entire magmatic-hydrothermal event. Therefore, whether the transient volcanic eruption or even a great earthquake can exert a significant impact on the relative long-term porphyry mineralization remains to be further explored.

3.2 Sources of ore-forming materials of PCDs

The ultimate source of metallogenic materials in PCDs (i.e., metals such as Cu, Mo and Au, and volatiles such as S, Cl and water) include three major geological end-members: The subducting oceanic crust, the upper mantle and the middle-upper crust. It is long regarded that Cu, Au and platinum group elements (PGEs) were likely originated from the mantle, Mo and Pb from the subducting slab or the crust, and S from the subducting slab (Seedorff et al., 2005). However, considering that the average Cu content in the oceanic crust (74 ppm for MORB) is higher than the primitive mantle (30 ppm) and the continental crust (27 ppm), partial melting simulation under different fO_2 suggests that the Cu content in the oceanic crust-derived melt under high fO_2 (FMQ+1.5) can be as high as 400 ppm, which is higher than those derived from the mantle peridotite and the lower crust. This implies that partial melting of the oceanic crust is more favorable for the PCD formation (Sun et al., 2015; Zhang et al., 2017; Figure 9). However, Os and O isotopic studies on the veined peridotite xenolith above the subduction zone revealed that the subducting slab contributed less than 10% of the Os to the mantle wedge, indicating that the Cu and Au may have originated mainly from the mantle. In other words, subduction may have only provided the fluids that extract metals from the mantle, rather than being a major ore-forming metal source (McInnes et al., 1999). The simulation also shows that the Cu content in the melt derived from low-degree (<20%) partial melting of the mantle under high fO_2 has exceeded the lower limit of that required for mineralization, e.g., 3% partial melting of the mantle can generate a melt with up to 300 ppm Cu, which is close to the maximum Cu content (400 ppm) in the adakitic rocks produced by partial melting of the oceanic crust. This indicates a possible genetic link between K-rich magmas (produced by low-degree partial melting of the mantle) and porphyry Cu mineralization.

Cenozoic large porphyry Cu-Mo deposits are mainly distributed in the eastern Pacific margin, but virtually absent in the western Pacific margin. Such pattern has been explained by the "oceanic hypoxia event" hypothesis and different subduction systems on the eastern and western Pacific margin (Sun et al., 2016). The high oxidation anomalies before the "oceanic anoxic event" may have resulted in high Mo concentrations in the seawater and marine (organic) se-

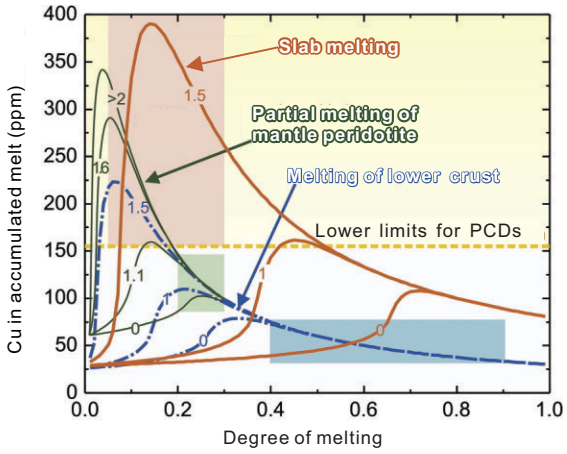

Figure 9 Cu content in the melt derived from the oceanic crust, mantle peridotite and lower crust versus the degree of partial melting under different fO_2 conditions. After Zhang et al. (2017).

diments, and the Mo was brought into the mantle wedge through the subducting slabs. In contrast, the limited distribution of large ocean basins in the western Pacific island arc environment restricts the input of terrestrial materials, resulting in lower Mo content in the sediments. In addition, the mineralization event is younger than the latest "oceanic hypoxia event", thus large porphyry Cu-Mo deposits are rarely formed in the western Pacific. However, given that the recent "oceanic anoxic event" occurred at 56 Ma, it is difficult to explain the formation of Neogene (mainly <35 Ma) porphyry Cu-Mo deposits in South America by the accumulation of Mo-rich organic sediments via surficial chemical weathering, which means that the continental arc lithosphere has a special mechanism to store and release Mo for mineralization.

The origin of S is an important and long-lasting problem for the PCD metallogenic studies. Mafic melt inclusion analysis in the Galunggung high-Mg basalt (Java, Indonesia) shows that S is significantly more enriched in the island arc mantle (cf. the depleted mantle), suggesting that the S may have entered the mantle wedge during slab dehydration (de Hoog et al., 2001; Li and Audétat, 2012). However, some authors have questioned that local composition of melt inclusions cannot fully reflect the overall S content of the mantle wedge. It is believed by many that the original island arc magma (high-Al basalt) and MORB have similar oxygen fugacity, i.e., they are not particularly S-rich (Lee et al., 2012). Meanwhile, the S enrichment mechanism via crustal magmatic evolution is still controversial: Some authors consider that the large S-flux necessary for PCD formation is derived from S-rich magma directly mixed with the ore-forming magma, or the injection of volatiles into the upper crustal magma chamber (Blundy et al., 2015). Melt inclusion analysis on the Bingham PCD indicates that the addition of S-rich magma provides the huge amount of S required for the mineralization (Zhang and Audétat, 2017). Meanwhile, many other authors consider that the magma may have become gradually S-rich with magmatic evolution in the crust, as supported by the large amount of magmatic anhydrite commonly found in the ore-forming rocks (Loucks, 2014; Hutchinson and Dilles, 2019). Therefore, the question remains unresolved.

3.3 Relative contributions of metal pre-enrichment in the magmatic sources and the evolutionary processes to mineralization

According to the geochemical transfer and tectonomagmatic processes at convergent plate boundaries (Zheng, 2019; Zheng et al., 2020), Zheng et al. (2019b) have proposed three stages of enrichment in ore-forming materials for the PCD formation. These include: (1) The initial enrichment of incompatible ore-forming elements in the subduction-zone fluids due to metamorphic dehydration and/or partial melting of the subducting oceanic crust; (2) further concentration of the ore-forming elements in the mafic melt formed by partial melting of the mantle wedge (metasomatized by subduction-zone fluids); (3) the final enrichment in ore-forming materials through fractional crystallization of the primary arc magmas, or partial melting of their crystallized product during magmatic evolution in the crust. In this regard, it is critical to evaluate the extent of metal enrichment in each stage. Hydrous amphibole cumulates in the lower crust are suggested as a favorable source for ore-forming magma, but the SCLM is also a candidate (Core et al., 2006; Richards, 2009; Griffin et al., 2013; Holwell et al., 2019).

Ordinary SCLM is often depleted in Au and Cu due to the high degree of partial melting of the upper mantle or strong liberation of metamorphic fluid in the deep crust (Hou et al., 2017). However, the fluid or melt derived from the subducting slab may enrich the mantle wedge or SCLM with ore-forming elements, and can activate the pre-enriched SCLM through low degree of partial melting, thus forming alkalic PCDs (Griffin et al., 2013). For example, the spatial distribution of the giant Au-rich PCDs and intrusion-related orogenic Au deposits in the western United States coincides with the enriched SCLM defined by low seismic velocity (Schmandt and Humphreys, 2010). Isotopic studies of these PCDs show Archean Pb isotope features in the ore fluids, suggesting that the second-stage enrichment may have occurred long after the first stage (Griffin et al., 2013). The reactivation does not necessarily require large-scale magmatism, but can also be achieved by local post-orogenic magmatism (Griffin et al., 2013; Zheng et al., 2019b). The Grasberg and Ok Tedi Au-rich PCDs, for example, were only connected to the Australian SCLM through crustal-scale faults, with no coeval large-scale magmatism (Hill et al., 2002).

Recent studies proposed that ore-forming, normal arc-type magmas may not require the first- and second-stage pre-enrichment (Richards, 2003; Audétat, 2015; Hou et al., 2015; Zhang and Audétat, 2017; Zheng et al., 2019a), but went through the third stage, i.e., transient but decisive crustal processes (Wilkinson, 2013). The key to resolve this dispute is to obtain samples that represent the original compositions of the crustal source region, such as ore-related xenoliths from the lower crustal cumulates, or the melt inclusions that represent the original composition before sulfide saturation in the upper crustal magma chamber. Recent studies on xenoliths and melt inclusions of PCDs, e.g., those on the Beiya PCD, show that the local Au and Cu concentrations in the lower crustal cumulates are higher than those of the normal arc magma. This suggests that the enriched lower crustal cumulates may have released the ore-forming materials into the parental magma in the later re-activation process. However, the analysis of amphibolite xenoliths from the middle and lower crustal source area of the Mujicun PCD (northern China) shows that the Cu content in the source area is similar to the average Cu content of the normal arc magmas, which means that there was no Cu enrichment in the magma source. Meanwhile, the sulfide dissolution features observed in the upper crustal gabbronorite of the PCD suggests that the magma may have begun concentrating the ore-forming materials in the upper crustal magma chamber(s) (Hou et al., 2015).

In the model of lower crust cumulates, local sulfide saturation occurs during the crystallization of water-rich magma, and the precipitated sulfide is captured between amphibole and other crystallized mineral phases, so as to extract some ore-forming materials for storage and retention in the lower crust. In the subsequent evolution, the rising geothermal gradient of magmatic arc (Davidson et al., 2007) and the recharge of mantle-derived magmas (Hou et al., 2017) may have heated and decomposed the amphibolite there, and produced abundant volatiles and ore-forming materials. Statistical studies on published arc magmatic rocks around the world found that the Cu content of arc magmas is inversely proportional to the crustal thickness (Chiaradia, 2014), i.e., lower in the thicker crust (>30 km) and higher in the thinner crust (<20 km). Considering the synchronous changes in Fe and Cu contents, we propose that magnetite crystallization may have caused sulfide precipitation, thus stripping Cu from the magma and accumulate sulfides at the bottom of the lower crust. However, it should be noted that the above study ignores the temporal evolution of island arcs and continental margin arcs, and fails to extract the age of the statistical geochemical data. The study may have mixed the magmatic data before/after the island arc thickening, and cannot reveal accurately the influence of crustal thickening on the geochemical compositions of ore-forming magma. Meanwhile, the magmas may have undergone shallow degassing or ore-material extraction, and cannot represent the original magma compositions. The second model suggests that the mixing of mafic and felsic magma may have resulted in local sulfide saturation in the magma chamber and formed isolated sulfide phases (Halter et al., 2005). However, this process does not necessarily cause the dilution of ore-forming elements in the magmas (Zhang and Audétat, 2017), because the later volatile phases may have decomposed the metal-rich sulfide phase and formed magmatic-hydrothermal mineralization. Previous studies have concluded that it is difficult for arc magmas to form magmatic Cu-Ni sulfide deposits. This is because arc magmas are commonly richer in volatiles than intra-plate magmas, which can decompose sulfide phase in mafic magma and form ore-element-rich magmatic-hydrothermal fluids, and facilitates the subsequent PCD mineralization (Nadeau et al., 2010; Edmonds et al., 2018).

The above two ore-forming element pre-enrichment models can explain the decoupling of Au and Cu and the formation of Au-rich PCDs. Previous studies have pointed out that the sulfide phase absorbs more Au than Cu from the magmas ($D_{Au}>D_{Cu}$), and then be re-mobilized by tectono-magmatic events in the lower crust to form Au-rich mineralization (Richards, 2009; Griffin et al., 2013). Alternatively, the sulfide phase can be completely decomposed by volatiles in the upper crust magma chamber as aforementioned, thus forming hydrothermal fluid with high Au/Cu ratio (Halter et al., 2002; Halter et al., 2005). It is noteworthy that in the melt inclusions from the Alumbrera PCD, the sulfide phase is separated into Fe-rich and Cu-rich one (Halter et al., 2002), and Au tends to enter the former. Although the sulfide phase in the upper crustal magma chamber is considered to be completely decomposed by volatiles (Halter et al., 2002; Halter et al., 2005), the Au/Cu ratios in the fluid inclusions (representing the volatiles) at the Bingham PCD are higher than those in the sulfide melt inclusions (Zhang and Audétat, 2017). This indicates that Au and Cu have more complex distribution behaviors between the volatile and sulfide melt phases. Therefore, we believe that the composition of the sulfide cumulates and their behaviors in the later hydrothermal process are the key controlling factors of Au and Cu differentiation.

The sulfide pre-enrichment model challenges the importance of a highly oxidized PCD ore-forming magma. Traditional PCD metallogenic models propose that the magma needs to maintain a high oxidation state to avoid the early formation of sulfide phase that scavenges ore-forming elements. However, isolated sulfide phase is common in the xenoliths of lower crustal cumulates (Richards, 2009; Hou et al., 2017). Sulfides droplets in the melt inclusions represent the components of the upper crustal magma chamber (Nadeau et al., 2010), suggesting that the sulfide saturation in the magma may be a common phenomenon. Geological observations and simulations also show that the volatiles have

become more oxidized due to adiabatic expansion during the magma ascent (i.e., decoupled from fO_2 of the melt; Oppenheimer et al., 2018), suggesting that the magma can produce a volatile phase (with higher fO_2 than the melt) that can decompose the early-formed sulfides. Instead of the lower or upper crustal storage model, we propose a continuous pre-enrichment model: The region extending from the bottom of the MASH zone to the upper crust mimics the "crystal mush" (Magee et al., 2018), where mineral crystallization and magma ponding and ascent occur continuously, and the magma ponding may be accompanied by continuous pre-enrichment of sulfides. This extreme pre-enrichment model may explain the fact that large PCDs are often formed in the late evolution stage of magmatic arcs, because the metal-rich cumulates there have greater metallogenic potential. In summary, the questions of whether the enrichment in the first and second stages is the premise of the third stage, whether there is any difference between common arc-type magma and ore-forming magma, what is the impact of the third-stage pre-enrichment on Au and Cu differentiation, how to identify and evaluate the pre-enrichment process of ore-forming materials in the crust, and what are the key issues (e.g., the activation mechanism and detailed process of sulfide pre-enrichment) should be further clarified in future research.

4. Concluding remarks

Based on the above PCD data compilation and analysis, we suggest that:

The origin of magma of PCD can be traced back to the dehydration or partial melting of subducted slab, which is accompanied by fluid or melt transporting oceanic crust material to the metasomatized mantle wedge. This results in the partial melting of the mantle to form high-Al basaltic magma, which represents the original island arc magma. Meanwhile, the adakitic melt, which is formed by partial melting of young hot oceanic crust or subducted oceanic ridge, interacts with the mantle peridotite in the mantle wedge and forms adakitic ore-forming magmas with mantle-derived affinities.

In mature island arcs or continental arcs, the magma formed by partial melting of the mantle intrudes into the hot zone around the crust-mantle boundary, and experiences complex crust-mantle interactions (MASH) to form the low-density andesitic-dacitic melt. When the water in the arc magma accumulates in the amphibole-stability field, extensive fractionation of amphibole and other mafic minerals forms the cumulate layer at the bottom of the lower crust, which captures the sulfide phase that may later participates in the PCD formation. The adakitic characteristics would be obtained by magma H_2O content increase in the MASH zone, resulted from the fractional crystallization of amphibole, the eclogite-facies metamorphism of the lower crust, and the subduction erosion of the magmatic arc front.

The compressive-extensional transition of the subduction zone likely promotes the rise of the ore-forming parental magma. The initial intermediate-felsic magmas generally ascend to the neutral buoyancy interface of the upper crust, accumulates to form magma chamber(s), and undergoes fractionation, magma replenishment, and fluid exsolution. Sulfide saturation may enrich the ore-forming elements more efficiently. The mafic magma is directly mixed or indirectly injected into the magma chamber by volatiles, supplying more ore-forming elements, including Cu, Au, Mo, and S.

Magma may intrude into the upper crust as apophysis or stock from the top of magma chamber at the bottom of the upper crust, forming various mineralized porphyries. "First boiling" is likely triggered by the collapse of the upper volcanic edifice, large earthquakes, rapid uplift and erosion, brittle-ductile regime fluctuations and mafic magma replenishment. In the early mineralization stage(s), supercritical fluids are likely rich in ore-forming elements, followed by the brine phase and gas phase. It is generally believed that Mo is mainly transported by the brine phase, and Au and half of Cu by the gas phase. In addition, the timing of saturation of single-phase volatiles or liquid brine from the magma chamber, salinity (Cl/H_2O), and oxygen fugacity are the primary controls for the subsequent hydrothermal mineralization.

The potassic alteration stage of PCDs is initially formed by the high-temperature single-phase fluid directly exsolved from the magma, and then rises and separates into the high-density brine and low-density gas phases, with the latter rising to form argillic alteration. Sericite alteration is mainly formed by the low-temperature liquid phase directly differentiated from the magmas. Meteoric water may be added to phyllic alteration at the periphery of the alteration system. Propylitic alteration is formed by mixing the magma-derived brine with groundwater, and may locally superimpose on the potassic zone in the late alteration stage. If the metals are transported in chlorite complexes, much homologous oxidized sulfur (SO_2 or SO_4^{2-}) is needed to be reduced, or addition of reduced S is needed to precipitate the ore sulfides; whereas if the metals are transported in bisulfide complexes, ore sulfide precipitation can be achieved through decompression and degassing of H_2S or fluid-wallrock reactions.

Acknowledgements *Constructive comments and suggestions by the Editor-in-Chief Yongfei Zheng and three anonymous reviewers greatly improved the manuscript. This is contribution No. IS-2745 from GIGCAS. This study was supported by the National Natural Science Foundation of China for Distinguished Young Scholars (Grant No. 41725009), the "135" Planned Project of Guangzhou Institute of Geochemistry, Chinese Academy of Sciences (Grant No.135PY201606) and the Strategic Priority Program of the Chinese Academy of Sciences (Type B) (Grant No. XDB18030206).*

References

Annen C, Blundy J D, Sparks R S J. 2005. The genesis of intermediate and silicic magmas in deep crustal hot zones. J Petrol, 47: 505–539

Ardill K, Paterson S, Memeti V. 2018. Spatiotemporal magmatic focusing in upper-mid crustal plutons of the Sierra Nevada arc. Earth Planet Sci Lett, 498: 88–100

Audétat A. 2015. Compositional evolution and formation conditions of magmas and fluids related to porphyry Mo mineralization at Climax, Colorado. J Petrol, 56: 1519–1546

Bissig T, Clark A H, Lee J K W, von Quadt A. 2003. Petrogenetic and metallogenetic responses to Miocene slab flattening: New constraints from the El Indio-Pascua Au-Ag-Cu belt, Chile/Argentina. Miner Depos, 38: 844–862

Blundy J, Mavrogenes J, Tattitch B, Sparks S, Gilmer A. 2015. Generation of porphyry copper deposits by gas-brine reaction in volcanic arcs. Nat Geosci, 8: 235–240

Bodinier J L, Menzies M A, Shimizu N, Frey F A, McPherson E. 2004. Silicate, hydrous and carbonate metasomatism at Lherz, France: Contemporaneous derivatives of silicate melt-harzburgite reaction. J Petrol, 45: 299–320

Buret Y, von Quadt A, Heinrich C, Selby D, Wälle M, Peytcheva I. 2016. From a long-lived upper-crustal magma chamber to rapid porphyry copper emplacement: Reading the geochemistry of zircon crystals at Bajo de la Alumbrera (NW Argentina). Earth Planet Sci Lett, 450: 120–131

Candela P A, Holland H D. 1986. A mass transfer model for copper and molybdenum in magmatic hydrothermal systems: The origin of porphyry-type ore deposits. Econ Geol, 81: 1–19

Candela P A, Piccoli P M. 2005. Magmatic processes in the development of porphyry-type ore systems. Econ Geol, 100: 25–38

Cannell J, Cooke D R, Walshe J L, Stein H. 2005. Geology, mineralization, alteration, and structural evolution of the El Teniente porphyry Cu-Mo deposit. Econ Geol, 100: 979–1003

Cao M J, Evans N J, Hollings P, Cooke D R, McInnes B I A, Qin K Z, Li G M. 2018a. Phenocryst zonation in porphyry-related rocks of the Baguio district, Philippines: Evidence for magmatic and metallogenic processes. J Petrol, 59: 825–848

Cao M J, Hollings P, Cooke D R, Evans N J, McInnes B I A, Qin K Z, Li G M, Sweet G, Baker M. 2018b. Physicochemical processes in the magma chamber under the Black Mountain porphyry Cu-Au deposit, Philippines: Insights from mineral chemistry and implications for mineralization. Econ Geol, 113: 63–82

Caricchi L, Annen C, Blundy J, Simpson G, Pinel V. 2014. Frequency and magnitude of volcanic eruptions controlled by magma injection and buoyancy. Nat Geosci, 7: 126–130

Castillo P R. 2006. An overview of adakite petrogenesis. Chin Sci Bull, 51: 268–257

Castillo P R, Janney P E, Solidum R U. 1999. Petrology and geochemistry of Camiguin Island, southern Philippines: Insights to the source of adakites and other lavas in a complex arc setting. Contrib Mineral Petrol, 134: 33–51

Cathles L M, Shannon R. 2007. How potassium silicate alteration suggests the formation of porphyry ore deposits begins with the nearly explosive but barren expulsion of large volumes of magmatic water. Earth Planet Sci Lett, 262: 92–108

Cernuschi F, Dilles J H, Grocke S B, Valley J W, Kitajima K, Tepley Frank J. I. 2018. Rapid formation of porphyry copper deposits evidenced by diffusion of oxygen and titanium in quartz. Geology, 46: 611–614

Chen W, Xiong X L, Wang J T, Xue S, Li L, Liu X C, Ding X, Song M S. 2018. TiO_2 solubility and Nb and Ta partitioning in rutile-silica-rich supercritical fluid systems: Implications for subduction zone processes. J Geophys Res-Solid Earth, 123: 4765–4782

Chiaradia M. 2014. Copper enrichment in arc magmas controlled by overriding plate thickness. Nat Geosci, 7: 43–46

Chiaradia M, Ulianov A, Kouzmanov K, Beate B. 2012. Why large porphyry Cu deposits like high Sr/Y magmas? Sci Rep, 2: 685

Cooke D R, Hollings P, Walshe J L. 2005. Giant porphyry deposits: Characteristics, distribution, and tectonic controls. Econ Geol, 100: 801–818

Cooke D R, Baker M, Hollings P, Sweet G, Chang Z, Danyushevsky L, Gilbert S, Zhou T, White N C, Gemmell J B. 2014. New advances in detecting the distal geochemical footprints of porphyry systems—Epidote mineral chemistry as a tool for vectoring and fertility assessments. Soc Econ Geol Spec Publ, 18: 1–27

Core D P, Kesler S E, Essene E J. 2006. Unusually Cu-rich magmas associated with giant porphyry copper deposits: Evidence from Bingham, Utah. Geology, 34: 41–44

Crerar D A, Barnes H L. 1976. Ore solution chemistry V. Solubilities of chalcopyrite and chalcocite assemblages in hydrothermal solution at 200°C to 350°C. Econ Geol, 71: 772–794

Dauphas N, Craddock P R, Asimow P D, Bennett V C, Nutman A P, Ohnenstetter D. 2009. Iron isotopes may reveal the redox conditions of mantle melting from Archean to Present. Earth Planet Sci Lett, 288: 255–267

Davidson J P. 1996. Deciphering mantle and crustal signatures in subduction zone magmatism. Geophys Monogr, 96: 251–262

Davidson J, Turner S, Handley H, MacPherson C, Dosseto A. 2007. Amphibole “sponge” in arc crust? Geology, 35: 787

Davis M, Koenders M A, Petford N. 2007. Vibro-agitation of chambered magma. J Volcanol Geotherm Res, 167: 24–36

de Hoog J C M, Mason P R D, van Bergen M J. 2001. Sulfur and chalcophile elements in subduction zones: Constraints from a laser ablation ICP-MS study of melt inclusions from Galunggung Volcano, Indonesia. Geochim Cosmochim Acta, 65: 3147–3164

Defant M J, Drummond M S. 1990. Derivation of some modern arc magmas by melting of young subducted lithosphere. Nature, 347: 662–665

DePaolo D J. 1981. Trace element and isotopic effects of combined wallrock assimilation and fractional crystallization. Earth Planet Sci Lett, 53: 189–202

Dilles J H. 1987. Petrology of the Yerington Batholith, Nevada: Evidence for evolution of porphyry copper ore fluids. Econ Geol, 82: 1750–1789

Ducea M N, Paterson S R, DeCelles P G. 2015. High-volume magmatic events in subduction systems. Elements, 11: 99–104

Edmonds M, Mather T A, Liu E J. 2018. A distinct metal fingerprint in arc volcanic emissions. Nat Geosci, 11: 790–794

Fekete S, Weis P, Driesner T, Bouvier A S, Baumgartner L, Heinrich C A. 2016. Contrasting hydrological processes of meteoric water incursion during magmatic-hydrothermal ore deposition: An oxygen isotope study by ion microprobe. Earth Planet Sci Lett, 451: 263–271

Fournier R O. 1999. Hydrothermal processes related to movement of fluid from plastic into brittle rock in the magmatic-epithermal environment. Econ Geol, 94: 1193–1211

Frank M R, Candela P A, Piccoli P M, Glascock M D. 2002. Gold solubility, speciation, and partitioning as a function of HCl in the brine-silicate melt-metallic gold system at 800°C and 100 MPa. Geochim Cosmochim Acta, 66: 3719–3732

Galvez M E, Connolly J A D, Manning C E. 2016. Implications for metal and volatile cycles from the pH of subduction zone fluids. Nature, 539: 420–424

Geiger S, Haggerty R, Dilles J H, Reed M H, Matthai S K. 2002. New insights from reactive transport modelling: The formation of the sericitic vein envelopes during early hydrothermal alteration at Butte, Montana. Geofluids, 2: 185–201

Glazner A F. 1991. Plutonism, oblique subduction, and continental growth: An example from the Mesozoic of California. Geology, 19: 784–786

Glazner A F, Bartley J M, Coleman D S, Gray W, Taylor R Z. 2004. Are plutons assembled over millions of years by amalgamation from small magma chambers? GSA Today, 14: 4

Griffin W L, Begg G C, O’Reilly S Y. 2013. Continental-root control on the genesis of magmatic ore deposits. Nat Geosci, 6: 905–910

Grove T L, Parman S W, Bowring S A, Price R C, Baker M B. 2002. The role of an H_2O-rich fluid component in the generation of primitive

basaltic andesites and andesites from the Mt. Shasta region, N California. Contrib Mineral Petrol, 142: 375–396
Gustafson L B, Hunt J P. 1975. The porphyry copper deposit at El Salvador, Chile. Econ Geol, 70: 857–912
Halter W E, Pettke T, Heinrich C A. 2002. The origin of Cu/Au ratios in porphyry-type ore deposits. Science, 296: 1844–1846
Halter W E, Heinrich C A, Pettke T. 2005. Magma evolution and the formation of porphyry Cu-Au ore fluids: Evidence from silicate and sulfide melt inclusions. Miner Depos, 39: 845–863
Harris A C, Golding S D. 2002. New evidence of magmatic-fluid-related phyllic alteration: Implications for the genesis of porphyry Cu deposits. Geology, 30: 335–338
Harrison R L, Maryono A, Norris M S, Rohrlach B D, Cooke D R, Thompson J M, Creaser R A, Thiede D S. 2018. Geochronology of the Tumpangpitu porphyry Au-Cu-Mo and high-sulfidation epithermal Au-Ag-Cu Deposit: Evidence for pre- and postmineralization diatremes in the Tujuh Bukit district, Southeast Java, Indonesia. Econ Geol, 113: 163–192
Hattori K H, Guillot S. 2003. Volcanic fronts form as a consequence of serpentinite dehydration in the forearc mantle wedge. Geology, 31: 525–528
Hedenquist J W, Lowenstern J B. 1994. The role of magmas in the formation of hydrothermal ore deposits. Nature, 370: 519–527
Hedenquist J W, Arribas A, Reynolds T J. 1998. Evolution of an intrusion-centered hydrothermal system: Far Southeast-Lepanto porphyry and epithermal Cu-Au deposits, Philippines. Econ Geol, 93: 373–404
Heinrich C A, Günther D, Audétat A, Ulrich T, Frischknecht R. 1999. Metal fractionation between magmatic brine and vapor, determined by microanalysis of fluid inclusions. Geology, 27: 755–758
Heinrich C A, Driesner T, Stefánsson A, Seward T M. 2004. Magmatic vapor contraction and the transport of gold from the porphyry environment to epithermal ore deposits. Geology, 32: 761–764
Henley R W, McNabb A. 1978. Magmatic vapor plumes and ground-water interaction in porphyry copper emplacement. Econ Geol, 73: 1–20
Hildreth W. 1981. Gradients in silicic magma chambers: Implications for lithospheric magmatism. J Geophys Res, 86: 10153–10192
Hildreth W, Moorbath S. 1988. Crustal contributions to arc magmatism in the Andes of Central Chile. Contr Mineral Petrol, 98: 455–489
Hill K C, Kendrick R D, Crowhurst P V, Gow P A. 2002. Copper-gold mineralisation in New Guinea: Tectonics, lineaments, thermochronology and structure. Aust J Earth Sci, 49: 737–752
Holland H D. 1972. Granites, solutions, and base metal deposits. Econ Geol, 67: 281–301
Hollings P, Cooke D R, Waters P J, Cousens B. 2011. Igneous geochemistry of mineralized rocks of the Baguio District, Philippines: Implications for tectonic evolution and the genesis of porphyry-style mineralization. Econ Geol, 106: 1317–1333
Hou Z Q. 2004. Porphyry Cu-Mo-Au deposits: Some new insights and advances. Earth Sci Front, 11: 131–144
Hou Z Q, Gao Y F, Meng X L, Qu X M, Huang M. 2004. Genesis of adakitic porphyry and tectonic controls on the Gangdese Miocene porphyry copper belt in the Tibetan orogen. Acta Petrol Sin, 20: 239–248
Hou Z Q, Yang Z M. 2009. Porphyry deposits in continental settings of China: Geological characteristics, magmatic-hydrothermal system, and metallogenic model. Acta Geol Sin, 83: 1779–1818
Hou Z Q, Yang Z M, Qu X M, Meng X J, Li Z Q, Beaudoin G, Rui Z Y, Gao Y F, Zaw K. 2009. The Miocene Gangdese porphyry copper belt generated during post-collisional extension in the Tibetan Orogen. Ore Geol Rev, 36: 25–51
Hou Z Q, Li Q Y, Gao Y F, Lu Y J, Yang Z M, Wang R, Shen Z C. 2015. Lower-crustal magmatic hornblendite in North China Craton: Insight into the genesis of porphyry Cu deposits. Econ Geol, 110: 1879–1904
Hou Z Q, Zhou Y, Wang R, Zheng Y C, He W Y, Zhao M, Evans N J, Weinberg R F. 2017. Recycling of metal-fertilized lower continental crust: Origin of non-arc Au-rich porphyry deposits at cratonic edges. Geology, 45: 563–566
Holwell D A, Fiorentini M, McDonald I, Lu Y, Giuliani A, Smith D J, Keith M, Locmelis M. 2019. A metasomatized lithospheric mantle control on the metallogenic signature of post-subduction magmatism. Nat Commun, 10: 3511
Hutchinson M C, Dilles J H. 2019. Evidence for magmatic anhydrite in porphyry copper intrusions. Econ Geol, 114: 143–152
Ingebritsen S E. 2012. Modeling the formation of porphyry-copper ores. Science, 338: 1551–1552
Ishihara S, Matsuhisa Y. 1999. Oxygen isotopic constraints on the geneses of the Miocene Outer Zone granitoids in Japan. Lithos, 46: 523–534
Jagoutz O, Müntener O, Ulmer P, Pettke T, Burg J P, Dawood H, Hussain S. 2007. Petrology and mineral chemistry of lower crustal intrusions: The Chilas Complex, Kohistan (NW Pakistan). J Petrol, 48: 1895–1953
Jenner F E, O'Neill H S C, Arculus R J, Mavrogenes J A. 2010. The magnetite crisis in the evolution of arc-related magmas and the initial concentration of Au, Ag and Cu. J Petrol, 51: 2445–2464
Jugo P J. 2009. Sulfur content at sulfide saturation in oxidized magmas. Geology, 37: 415–418
Kay R W. 1978. Aleutian magnesian andesites: Melts from subducted Pacific Ocean crust. J Volcanol Geotherm Res, 4: 117–132
Kay S M, Mpodozis C. 2001. Central Andean ore deposits linked to evolving shallow subduction systems and thickening crust. Geol Soc Am Today, 11: 4–9
Kay S M, Godoy E, Kurtz A. 2005. Episodic arc migration, crustal thickening, subduction erosion, and magmatism in the south-central Andes. Geol Soc Am Bull, 117: 67–88
Keith J D, Whitney J A, Hattori K, Ballantyne G H, Christiansen E H, Barr D L, Cannan T M, Hook C J. 1997. The role of magmatic sulfides and mafic alkaline magmas in the Bingham and Tintic mining districts, Utah. J Petrol, 38: 1679–1690
Kelley K A, Cottrell E. 2009. Water and the oxidation state of subduction zone magmas. Science, 325: 605–607
Kent A J R, Peate D W, Newman S, Stolper E M, Pearce J A. 2002. Chlorine in submarine glasses from the Lau Basin: Seawater contamination and constraints on the composition of slab-derived fluids. Earth Planet Sci Lett, 202: 361–377
Kerrick D M, Connolly J A D. 2001. Metamorphic devolatilization of subducted oceanic metabasalts: Implications for seismicity, arc magmatism and volatile recycling. Earth Planet Sci Lett, 189: 19–29
Kessel R, Schmidt M W, Ulmer P, Pettke T. 2005. Trace element signature of subduction-zone fluids, melts and supercritical liquids at 120–180 km depth. Nature, 437: 724–727
Landtwing M R, Pettke T, Halter W E, Heinrich C A, Redmond P B, Einaudi M T, Kunze K. 2005. Copper deposition during quartz dissolution by cooling magmatic-hydrothermal fluids: The Bingham porphyry. Earth Planet Sci Lett, 235: 229–243
Large S J E, Quadt A, Wotzlaw J F, Guillong M, Heinrich C A. 2018. Magma evolution leading to porphyry Au-Cu mineralization at the Ok Tedi deposit, Papua New Guinea: Trace element geochemistry and high-precision geochronology of igneous zircon. Econ Geol, 113: 39–61
Lee C T A, Luffi P, Chin E J, Bouchet R, Dasgupta R, Morton D M, Le Roux V, Yin Q, Jin D. 2012. Copper systematics in arc magmas and implications for crust-mantle differentiation. Science, 336: 64–68
Leeman W P. 2001. The influence of subduction zone thermal structure on arc magma chemistry: B and fluid-mobile elements. AGU Fall Meeting Abstracts
Lerchbaumer L, Audétat A. 2012. High Cu concentrations in vapor-type fluid inclusions: An artifact? Geochim Cosmochim Acta, 88: 255–274
Li Y, Audétat A, Lerchbaumer L, Xiong X L. 2009. Rapid Na, Cu exchange between synthetic fluid inclusions and external aqueous solutions: Evidence from LA-ICP-MS analysis. Geofluids, 9: 321–329
Li Y, Audétat A. 2012. Partitioning of V, Mn, Co, Ni, Cu, Zn, As, Mo, Ag, Sn, Sb, W, Au, Pb, and Bi between sulfide phases and hydrous basanite melt at upper mantle conditions. Earth Planet Sci Lett, 355-356: 327–340
Ling M X, Wang F Y, Ding X, Zhou J B, Sun W. 2011. Different origins of adakites from the Dabie Mountains and the Lower Yangtze River Belt, eastern China: Geochemical constraints. Int Geol Rev, 53: 727–740

Liu H T, Zhang Q, Liu J M, Ye J, Zeng Q D, Yu C M. 2004. Adakite versus porphyry copper and epithermal gold deposit: A possible metallogenetic specialization of magmatism required in-deep assessment. Acta Petrol Sin, 20: 205–218
Liu S A, Li S, He Y, Huang F. 2010. Geochemical contrasts between early Cretaceous ore-bearing and ore-barren high-Mg adakites in central-eastern China: Implications for petrogenesis and Cu-Au mineralization. Geochim Cosmochim Acta, 74: 7160–7178
Loucks R R. 2014. Distinctive composition of copper-ore-forming arc-magmas. Aust J Earth Sci, 61: 5–16
Lowell J D, Guilbert J M. 1970. Lateral and vertical alteration-mineralization zoning in porphyry ore deposits. Econ Geol, 65: 373–408
Lowenstern J. 2001. Carbon dioxide in magmas and implications for hydrothermal systems. Miner Depos, 36: 490–502
Luhr J F. 1997. Extensional tectonics and the diverse primitive volcanic rocks in the western Mexican Volcanic Belt. Can Mineral, 35: 473–500
Magee C, Stevenson C T E, Ebmeier S K, Keir D, Hammond J O S, Gottsmann J H, Whaler K A, Schofield N, Jackson C A L, Petronis M S, O'Driscoll B, Morgan J, Cruden A, Vollgger S A, Dering G, Micklethwaite S, Jackson M D. 2018. Magma plumbing systems: A geophysical perspective. J Petrol, 59: 1217–1251
Marschall H R, Schumacher J C. 2012. Arc magmas sourced from mélange diapirs in subduction zones. Nat Geosci, 5: 862–867
Maryono A, Harrison R L, Cooke D R, Rompo I, Hoschke T G. 2018. Tectonics and geology of porphyry Cu-Au deposits along the Eastern Sunda magmatic arc, Indonesia. Econ Geol, 113: 7–38
McInnes B I A, McBride J S, Evans N J, Lambert D D, Andrew A S. 1999. Osmium isotope constraints on ore metal recycling in subduction zones. Science, 286: 512–516
Mpodozis C, Cornejo P. 2012. Cenozoic tectonics and porphyry copper systems of the Chilean Andes. Soc Econ Geol Spec Publ, 16: 329–360
Mungall J E. 2002. Roasting the mantle: Slab melting and the genesis of major Au and Au-rich Cu deposits. Geology, 30: 915–918
Müntener O, Kelemen P B, Grove T L. 2001. The role of H_2O during crystallization of primitive arc magmas under uppermost mantle conditions and genesis of igneous pyroxenites: An experimental study. Contrib Mineral Petrol, 141: 643–658
Nadeau O, Williams-Jones A E, Stix J. 2010. Sulphide magma as a source of metals in arc-related magmatic hydrothermal ore fluids. Nat Geosci, 3: 501–505
Nagaseki H, Hayashi K I. 2008. Experimental study of the behavior of copper and zinc in a boiling hydrothermal system. Geology, 36: 27–30
Noll Jr P D, Newsom H E, Leeman W P, Ryan J G. 1996. The role of hydrothermal fluids in the production of subduction zone magmas: Evidence from siderophile and chalcophile trace elements and boron. Geochim Cosmochim Acta, 60: 587–611
O'Neill H S C, Mavrogenes J A. 2002. The sulfide capacity and the sulfur content at sulfide saturation of silicate melts at 1400°C and 1 bar. J Petrol, 43: 1049–1087
Oppenheimer C, Scaillet B, Woods A, Sutton A J, Elias T, Moussallam Y. 2018. Influence of eruptive style on volcanic gas emission chemistry and temperature. Nat Geosci, 11: 678–681
Oyarzun R, Márquez A, Lillo J, López I, Rivera S. 2001. Giant versus small porphyry copper deposits of Cenozoic age in northern Chile: Adakitic versus normal calc-alkaline magmatism. Miner Depos, 36: 794–798
Pagé L, Hattori K, Guillot S. 2018. Mantle wedge serpentinites: A transient reservoir of halogens, boron, and nitrogen for the deeper mantle. Geology, 46: 883–886
Peach C L, Mathez E A, Keays R R. 1990. Sulfide melt-silicate melt distribution coefficients for noble metals and other chalcophile elements as deduced from MORB: Implications for partial melting. Geochim Cosmochim Acta, 54: 3379–3389
Pearce J A, Stern R J, Bloomer S H, Fryer P. 2005. Geochemical mapping of the Mariana arc-basin system: Implications for the nature and distribution of subduction components. Geochem Geophys Geosyst, 6: Q07006
Perelló J, Sillitoe R, Mpodozis C, Brockway H, Posso H. 2012. Geologic setting and evolution of the porphyry copper-molybdenum and copper-gold deposits at Los Pelambres, central Chile. Soc Econ Geol, 16: 79–104
Petford N, Kerr R C, Lister J R. 1993. Dike transport of granitoid magmas. Geology, 21: 845–848
Petford N, Cruden A R, McCaffrey K J W, Vigneresse J L. 2000. Granite magma formation, transport and emplacement in the Earth's crust. Nature, 408: 669–673
Pokrovski G S, Borisova A Y, Harrichoury J C. 2008. The effect of sulfur on vapor-liquid fractionation of metals in hydrothermal systems. Earth Planet Sci Lett, 266: 345–362
Pollard P, Taylor R. 2002. Paragenesis of the Grasberg Cu-Au deposit, Irian Jaya, Indonesia: Results from logging section 13. Miner Depos, 37: 117–136
Qian G, Brugger J, Skinner W M, Chen G, Pring A. 2010. An experimental study of the mechanism of the replacement of magnetite by pyrite up to 300°C. Geochim Cosmochim Acta, 74: 5610–5630
Reich M, Parada M A, Palacios C, Dietrich A, Schultz F, Lehmann B. 2003. Adakite-like signature of Late Miocene intrusions at the Los Pelambres giant porphyry copper deposit in the Andes of central Chile: Metallogenic implications. Miner Depos, 38: 876–885
Ribeiro J M, Maury R C, Grégoire M. 2016. Are adakites slab melts or high-pressure fractionated mantle melts? J Petrol, 57: 839–862
Richards J P. 2018. A shake-up in the porphyry world? Econ Geol, 113: 1225–1233
Richards J P. 2003. Tectono-magmatic precursors for porphyry Cu-(Mo-Au) deposit formation. Econ Geol, 98: 1515–1533
Richards J P. 2009. Postsubduction porphyry Cu-Au and epithermal Au deposits: Products of remelting of subduction-modified lithosphere. Geology, 37: 247–250
Richards J P, Spell T, Rameh E, Razique A, Fletcher T. 2012. High Sr/Y magmas reflect arc maturity, high magmatic water content, and porphyry Cu±Mo±Au potential: Examples from the Tethyan arcs of central and eastern Iran and western Pakistan. Econ Geol, 107: 295–332
Robb L. 2009. Introduction to Ore-Forming Processes. Hoboken: John Wiley & Sons
Roedder E. 1984. Fluid Inclusions. Mineralogical Society of America
Rusk B G, Reed M H, Dilles J H, Klemm L M, Heinrich C A. 2004. Compositions of magmatic hydrothermal fluids determined by LA-ICP-MS of fluid inclusions from the porphyry copper-molybdenum deposit at Butte, MT. Chem Geol, 210: 173–199
Rusk B G, Reed M H, Dilles J H. 2008. Fluid inclusion evidence for magmatic-hydrothermal fluid evolution in the porphyry copper-molybdenum deposit at Butte, Montana. Econ Geol, 103: 307–334
Schiano P, Clocchiatti R. 1994. Worldwide occurrence of silica-rich melts in sub-continental and sub-oceanic mantle minerals. Nature, 368: 621–624
Schilling F R, Partzsch G M. 2001. Quantifying partial melt fraction in the crust beneath the central Andes and the Tibetan Plateau. Phys Chem Earth Part A-Solid Earth Geod, 26: 239–246
Schmandt B, Humphreys E. 2010. Complex subduction and small-scale convection revealed by body-wave tomography of the western United States upper mantle. Earth Planet Sci Lett, 297: 435–445
Schoene B, Schaltegger U, Brack P, Latkoczy C, Stracke A, Günther D. 2012. Rates of magma differentiation and emplacement in a ballooning pluton recorded by U-Pb TIMS-TEA, Adamello batholith, Italy. Earth Planet Sci Lett, 355-356: 162–173
Seedorff E, Dilles J, Proffett J, Einaudi M, Zurcher L, Stavast W, Johnson D, Barton M. 2005. Porphyry deposits: Characteristics and origin of hypogene features. Econ Geol, 29: 251–298
Seo J H, Heinrich C A. 2013. Selective copper diffusion into quartz-hosted vapor inclusions: Evidence from other host minerals, driving forces, and consequences for Cu-Au ore formation. Geochim Cosmochim Acta, 113: 60–69
Sheppard S M F. 1977. Identification of the origin of oreforming solutions by the use of stable isotopes. Geol Soc Lond Spec Publ, 7: 25–41
Shinohara H, Kazahaya K, Lowenstern J B. 1995. Volatile transport in a

convecting magma column: Implications for porphyry Mo mineralization. Geology, 23: 1091–1094
Sillitoe R H. 1994. Erosion and collapse of volcanoes: Causes of telescoping in intrusion-centered ore deposits. Geology, 22: 945–948
Sillitoe R H. 1997. Characteristics and controls of the largest porphyry copper-gold and epithermal gold deposits in the circum-Pacific region. Aust J Earth Sci, 44: 373–388
Sillitoe R H. 2010. Porphyry copper systems. Econ Geol, 105: 3–41
Sillitoe R H. 2018. Why no porphyry copper deposits in Japan and South Korea? Resour Geol, 68: 107–125
Sillitoe R H, Perelló J. 2005. Andean copper province: Tectonomagmatic settings, deposit types, metallogeny, exploration, and discovery. Econ Geol 100th Anniv Volume. 845–890
Simon A C, Frank M R, Pettke T, Candela P A, Piccoli P M, Heinrich C A. 2005. Gold partitioning in melt-vapor-brine systems. Geochim Cosmochim Acta, 69: 3321–3335
Smith C M, Canil D, Rowins S M, Friedman R. 2012. Reduced granitic magmas in an arc setting: The Catface porphyry Cu-Mo deposit of the Paleogene Cascade Arc. Lithos, 154: 361–373
Sobolev A V, Chaussidon M. 1996. H_2O concentrations in primary melts from supra-subduction zones and mid-ocean ridges: Implications for H_2O storage and recycling in the mantle. Earth Planet Sci Lett, 137: 45–55
Sparks R S J, Marshall L A. 1986. Thermal and mechanical constraints on mixing between mafic and silicic magmas. J Volcanol Geotherm Res, 29: 99–124
Sparks R S J, Cashman K V. 2017. Dynamic magma systems: Implications for forecasting volcanic activity. Elements, 13: 35–40
Steinberger I, Hinks D, Driesner T, Heinrich C A. 2013. Source plutons driving porphyry copper ore formation: Combining geomagnetic data, thermal constraints, and chemical mass balance to quantify the magma chamber beneath the Bingham Canyon deposit. Econ Geol, 108: 605–624
Stern C R, Skewes M A, Arevalo A. 2010. Magmatic evolution of the giant El Teniente Cu-Mo deposit, central Chile. J Petrol, 52: 1591–1617
Sun W D, Zhang H, Ling M X, Ding X, Chung S L, Zhou J B, Yang X Y, Fan W M. 2011. The genetic association of adakites and Cu-Au ore deposits. Int Geol Rev, 53: 691–703
Sun W D, Huang R F, Li H, Hu Y B, Zhang C C, Sun S J, Zhang L P, Ding X, Li C Y, Zartman R E. 2015. Porphyry deposits and oxidized magmas. Ore Geol Rev, 65: 97–131
Sun W D, Li C Y, Hao X L, Ling M X, Ireland T, Ding X, Fan W M. 2016. Oceanic anoxic events, subduction style and molybdenum mineralization. Solid Earth Sci, 1: 64–73
Sun X, Lu Y J, McCuaig T C, Zheng Y Y, Chang H F, Guo F, Xu L J. 2018. Miocene ultrapotassic, high-Mg dioritic, and adakite- like rocks from Zhunuo in southern Tibet: Implications for mantle metasomatism and porphyry copper mineralization in collisional orogens. J Petrol, 59: 341–386
Tatsumi Y, Hamilton D L, Nesbitt R W. 1986. Chemical characteristics of fluid phase released from a subducted lithosphere and origin of arc magmas: Evidence from high-pressure experiments and natural rocks. J Volcanol Geotherm Res, 29: 293–309
Ulrich T, Heinrich C A. 2002. Geology and alteration geochemistry of the porphyry Cu-Au deposit at Bajo de la Alumbrera, Argentina. Econ Geol, 97: 1865–1888
Ulrich T, Mavrogenes J. 2008. An experimental study of the solubility of molybdenum in H_2O and KCl-H_2O solutions from 500°C to 800°C, and 150 to 300 MPa. Geochim Cosmochim Acta, 72: 2316–2330
Uyeda S, Kanamori H. 1979. Back-arc opening and the mode of subduction. J Geophys Res, 84: 1049–1061
Walker J A, Roggensack K, Patino L C, Cameron B I, Matías O. 2003. The water and trace element contents of melt inclusions across an active subduction zone. Contrib Mineral Petrol, 146: 62–77
Wang Q, Zhao Z H, Bao Z W, Xu J F, Liu W, Li C F, Bai Z H, Xiong X L. 2004. Geochemistry and petrogenesis of the Tongshankou and Yinzu adakitic intrusive rocks and the associated porphyry copper-molybdenum mineralization in southeast Hubei, East China. Resour Geol, 54: 137–152
Wark D A, Hildreth W, Spear F S, Cherniak D J, Watson E B. 2007. Pre-eruption recharge of the Bishop magma system. Geology, 35: 235–238
Weinberg R F, Podladchikov Y. 1994. Diapiric ascent of magmas through power law crust and mantle. J Geophys Res, 99: 9543–9559
Weis P, Driesner T, Heinrich C A. 2012. Porphyry-copper ore shells form at stable pressure-temperature fronts within dynamic fluid plumes. Science, 338: 1613–1616
Whattam S A, Stern R J. 2016. Arc magmatic evolution and the construction of continental crust at the Central American Volcanic Arc system. Int Geol Rev, 58: 653–686
Wilkinson J J. 2013. Triggers for the formation of porphyry ore deposits in magmatic arcs. Nat Geosci, 6: 917–925
Williams-Jones A E, Heinrich C A. 2005. 100th Anniversary special paper: Vapor transport of metals and the formation of magmatic-hydrothermal ore deposits. Econ Geol, 100: 1287–1312
Yokoi K, Matsubayashi N, Miyanaga T, Watanabe I, Ikeda S. 1993. Studies on the structure of molybdenum (VI) in acidic solution by xanes and exafs. Polyhedron, 12: 911–914
Zajacz Z, Hanley J J, Heinrich C A, Halter W E, Guillong M. 2009. Diffusive reequilibration of quartz-hosted silicate melt and fluid inclusions: Are all metal concentrations unmodified? Geochim Cosmochim Acta, 73: 3013–3027
Zajacz Z, Candela P A, Piccoli P M. 2017. The partitioning of Cu, Au and Mo between liquid and vapor at magmatic temperatures and its implications for the genesis of magmatic-hydrothermal ore deposits. Geochim Cosmochim Acta, 207: 81–101
Zhai Y S, Yao S Z, Cai K Q. 2011. Mineral Deposits. Beijing: Geological Publishing House
Zhang C C, Sun W D, Wang J T, Zhang L P, Sun S J, Wu K. 2017. Oxygen fugacity and porphyry mineralization: A zircon perspective of Dexing porphyry Cu deposit, China. Geochim Cosmochim Acta, 206: 343–363
Zhang D H, Audétat A. 2017. What caused the formation of the giant Bingham Canyon porphyry Cu-Mo-Au deposit? Insights from melt inclusions and magmatic sulfides. Econ Geol, 112: 221–244
Zhang Q, Wang Y, Qian Q, Yang J H, Wang Y L, Zhao T P, Guo G J. 2001. The characteristics and tectonic-metallogenic significances of the adakites in Yanshan period from eastern China. Acta Petrol Sin, 17: 236–244
Zheng Y C, Liu S A, Wu C D, Griffin W L, Li Z Q, Xu B, Yang Z M, Hou Z Q, O'Reilly S Y. 2019a. Cu isotopes reveal initial Cu enrichment in sources of giant porphyry deposits in a collisional setting. Geology, 47: 135–138
Zheng Y F. 2019. Subduction zone geochemistry. Geosci Front, 10: 1223–1254
Zheng Y F, Chen Y X, Dai L Q, Zhao Z F. 2015. Developing plate tectonics theory from oceanic subduction zones to collisional orogens. Sci China Earth Sci, 58: 1045–1069
Zheng Y F, Chen R X, Xu Z, Zhang S B. 2016. The transport of water in subduction zones. Sci China Earth Sci, 59: 651–682
Zheng Y F, Mao J W, Chen Y J, Sun W D, Ni P, Yang X Y. 2019b. Hydrothermal ore deposits in collisional orogens. Chin Sci Bull, 64: 205–212
Zheng Y F, Xu Z, Chen L, Dai L Q, Zhao Z F. 2020. Chemical geodynamics of mafic magmatism above subduction zones. J Asian Earth Sci, https://doi.org/10.1016/j.jseaes.2019.104185
Zhong R C, Brugger J, Chen Y J, Li W B. 2015. Contrasting regimes of Cu, Zn and Pb transport in ore-forming hydrothermal fluids. Chem Geol, 395: 154–164

(Responsible editor: Yongfei ZHENG)